

THESIS
CR11P
1960
C.2

**PETROGRAPHIC STUDY AND COMPOSITION ANALYSIS OF OLIVINE
PHENOCRYSTS FROM THE PAREA MESA BASALT FLOW,
BERNALILLO COUNTY, NEW MEXICO**

by

John H. Carman

7 2655

N.M.I.M.T.
LIBRARY
SUCCESSION

**Submitted in partial fulfillment for the degree of
Master of Science in Earth Science**

The New Mexico Institute of Mining and Technology

1960

134
Car
Cop. 2

This thesis is accepted on behalf of the
graduate faculty of the Institute by the following
committee:

Clay T. Smith
A. J. Budding
Charles A. Holmes
Edwin C. Coddige
Robert H. Walker

Date:

May 17, 1960

CONTENTS

	<u>Page</u>
Introduction	1
General Geology	2
Structure	11
Sampling	16
Laboratory Study	18
Hand Specimen Study	18
Thin-Section Analysis	22
X-ray Investigation of the Olivine Phenocryst Fraction	36
Analysis of X-ray Data	42
Summary	77
Conclusions	78
References	84

LIST OF ILLUSTRATIONS

Page

TABLES

1. Modal analysis of the Parea Mesa basalt	24
2. X-ray diffraction data for compositional determination of Parea Mesa olivine phenocrysts	44
3. X-ray diffraction data for composition determination of Buell Park olivine	49
4. Slope analysis of figure 5	51
5. X-ray compositions obtained in the first four oscillations for statistical analysis of data	57
6. Statistical comparison of data at the 90 percent confidence level	71

FIGURES

1. Geologic map of the Parea Mesa basalt	4
2. Isopach map of flows QTb ₁ and QTb ₂	13
3. Determination curve for olivine	43
4. Olivine sample composition means plotted against sample locality	52
5. Olivine sample composition means plotted with respect to sample position and locality	53
6. Histograms of olivine sample composition means plotted with respect to sample position	56

FIGURES (continued)

	<u>Page</u>
7. Histograms for the first four oscillations of samples from QTb ₂ plotted with respect to position	60
8. Histogram for the first four oscillations of samples from QTb ₂	62
9. Histograms of oscillations for mounts 1 and 2 of Buell Park olivine	68
10. Histogram of all oscillations of Buell Park olivine	69

PLATES

Plate 1.

A. View of Parea Mesa basalt, volcanic sediments and Quaternary gravel near sample locality 2	5
B. Pinch out of QTb ₁ and overlap of QTb ₂ near sample locality 2	5

Plate 2.

A. View of QTb ₂ and Qts near sample locality 6.	7
B. View of spheroidal zone in QTb ₂ near sample locality 10	7

Plate 3.

A. View of truncation in QTs near sample locality 5	8
B. View of transected axial portion of the northern portion of the Parea Mesa basin near sample locality 6	8

Plate 4.

A. Photograph of hand specimen showing spheroidal zone	20
--	----

	<u>Page</u>
B. Photograph of longitudinally cut surface of spheroidal zone	20
Plate 5.	
A. Photomicrograph of altered olivine in an unaltered intergranular groundmass, plane-polarized light	26
B. Same as A, crossed nicols	26
Plate 6.	
A. Photomicrograph of locale of intense alteration, plane-polarized light	29
B. Enlargement of A	29
Plate 7. Photomicrograph of pseudomorph after olivine	30
Plate 8.	
A. Photomicrograph, plane-polarized light, illustrating the occurrence and distribution of red alteration products	35
B. Enlargement of A	35
C. Photomicrograph, plane-polarized light, illustrating the occurrence and distribution of green alteration products	35
D. Enlargement of C	35

ABSTRACT

The purpose of this study was to investigate the variations in petrography and mineralogy of a single olivine bearing basalt flow. Particular attention was directed toward the composition of olivine found in the phenocryst fraction.

Samples were obtained from outcrops of the Parea Mesa basalt flows over a length of approximately 15,000 feet, 13,000 feet of which was restricted to a single flow. Utilizing a sample interval of approximately 1,000 feet, four samples were obtained from each sample locality. Chip samples were taken at 6-inch intervals from the base to the top of the flow and were combined into a single composite sample. In addition, grab samples of 1 to 2 pounds were taken from the top, middle and bottom of the flow.

The outcrops of the two lower flows of Parea Mesa basalt were found to be conformable to underlying volcanic sediments. These volcanic sediments are composed of two units of similar lithology but sharply divergent attitudes; the lower with a gentle eastward dip, and the upper with a steep westwardly dip which truncates the lower. The upper unit delineates a structural depression called the Parea Mesa basin. Field evidence indicates that

flow QTb₁ is restricted to the southern portion of this basin, whereas flow QTb₂ occupies the northern portion and also overlies beds of the lower volcanic sedimentary unit farther to the north and east.

Laboratory studies of hand specimens and thin-sections indicate that the Parea Mesa basalt is porphyritic to glomeroporphyritic olivine basalt. The color of the fresh surface, the structure and the type alteration all vary with regard to position in the flow. Spheroidal zones are an unusual feature of flow QTb₂, in which they are loci of most intense alteration. Green alteration products, montmorillonite, vermiculite and chlorite, are common in these zones, but locally they are changed by oxidation(?) into iddingsite-like red alteration products. Similar green alteration is found in the middle portion of the flow, although the alteration is less intense.

The compositions of olivine phenocrysts in the samples obtained were determined using the method and formula of Yoder and Sahama (1957). Statistical analysis of the olivine compositions reveals that lateral and vertical variations in flow QTb₂ are insignificant and the entire flow contains a single population of olivine with 77.5 ± 2.0 mol percent forsterite. A possible exception to this generalization is found in the olivine compositions of spheroidal zones; this population, represented by four samples, differs from the chip, bottom, top and flow composition populations of QTb₂ at confidence levels of 90 to 82 percent. However, the composition population of olivine from the

middle of the flow corresponds to spheroidal zone composition at all confidence levels greater than 59 percent. Thus, spheroidal zones and central portions of the flow are similar in both phenocryst composition and types of alteration, differing only in the intensity of alteration. The forsterite content of the olivine phenocryst composition varies inversely with the intensity of alteration. Spheroidal zones are thought to be caused by autolithic inclusions, by retention of deuteric solutions or both, however, no explanation can be offered for the difference in olivine composition from these zones.

Statistical comparisons drawn between the other sampled flows of Parca Mesa do not indicate any significant differences in the olivine compositions. A limited number of samples from other localities in New Mexico suggest that the evaluation of olivine compositions may be an important supplement to petrographic study of olivine bearing extrusives.

ACKNOWLEDGMENTS

The author was fortunate and is indeed grateful for the opportunity to discuss his program in its formative stages with Dr. Frederick J. Kuellmer and Dr. Robert Weber of the New Mexico Bureau of Mines and Mineral Resources, and with Dr. Clay T. Smith of the New Mexico Institute of Mining and Technology. Thanks are gratefully extended to Dr. Weber and Dr. Smith who read the manuscript and offered many helpful suggestions. Dr. Smith was of great assistance in his advisory capacity and the author is thankful for his understanding and interest.

Acknowledgment is also made to other members of the Institute and Bureau of Mines for stimulating and critical discussion on the program. In particular the author is indebted to Mr. A. J. Thompson, Director of the New Mexico Bureau of Mines and Mineral Resources, for the equipment, space, and materials provided for this study. A generous grant from the New Mexico Geological Society was most helpful in defraying the cost of materials, drafting, and typing.

INTRODUCTION

The difficulty of correlating basalts and other fine-grained volcanic rocks has long been a problem, and various solutions have been attempted. Among the first devised was Mathew's (1951) fusion method. Callaghan and Sun (1956) have used this method for the correlation of some igneous rocks of New Mexico, and recently Wargo (1960) has presented a somewhat modified technique based on magnetic susceptibility. To the author's knowledge these methods have not been used to study the variations, vertical or lateral, in individual flows. The author studied the lateral and vertical variations in one flow, as reflected in thin sections and the x-ray composition of phenocryst olivine, and compared the results with other flows of similar mineralogic composition.

The Parea Mesa flows in Bernalillo County, New Mexico were chosen as the sampling area for this investigation. This area was selected because of the rock type present (olivine-bearing basalt), and because of the extensive outcrop over which a single flow could be sampled and studied. Continuous chip samples and grab samples were collected in order to investigate variations that might exist in one flow. The composition of olivine phenocrysts was evaluated by means of statistical analysis.

GENERAL GEOLOGY

Parea Mesa is in the north-central portion of the Albuquerque-Belen basin of the Rio Grande structural depression. The field area is approximately one mile northwest of Isleta Pueblo, on the west side of New Mexico State Highway 45 (Coors Road).

The general geology and location of the Parea Mesa field area is shown in figure 1. No attempt was made to extend mapping to detailed features of the underlying volcanic sediments or to outer remnants of basalt close to Coors road and near Isleta Pueblo. Mapping was done on a topographic base (Isleta quadrangle); aerial photographs of the area were not available because of security restrictions.

Previous work in this area is limited to that of Wright (1946, p. 412) who states,

"Acuma Hill (topographically referred to as Parea Mesa), west of Isleta on the Rio Grande, is an exhumed lava cone surrounded by at least 50 feet of deformed, water-laid basaltic gravel overlain by 10 to 40 feet of lava, which is probably late Santa Fe. The Pueblo of Isleta is built upon the lava."

The water-laid basaltic gravel which Wright mentions is the oldest unit shown on figure 1, and is herein called volcanic sediment. The general field relations of the volcanic sediments are shown in

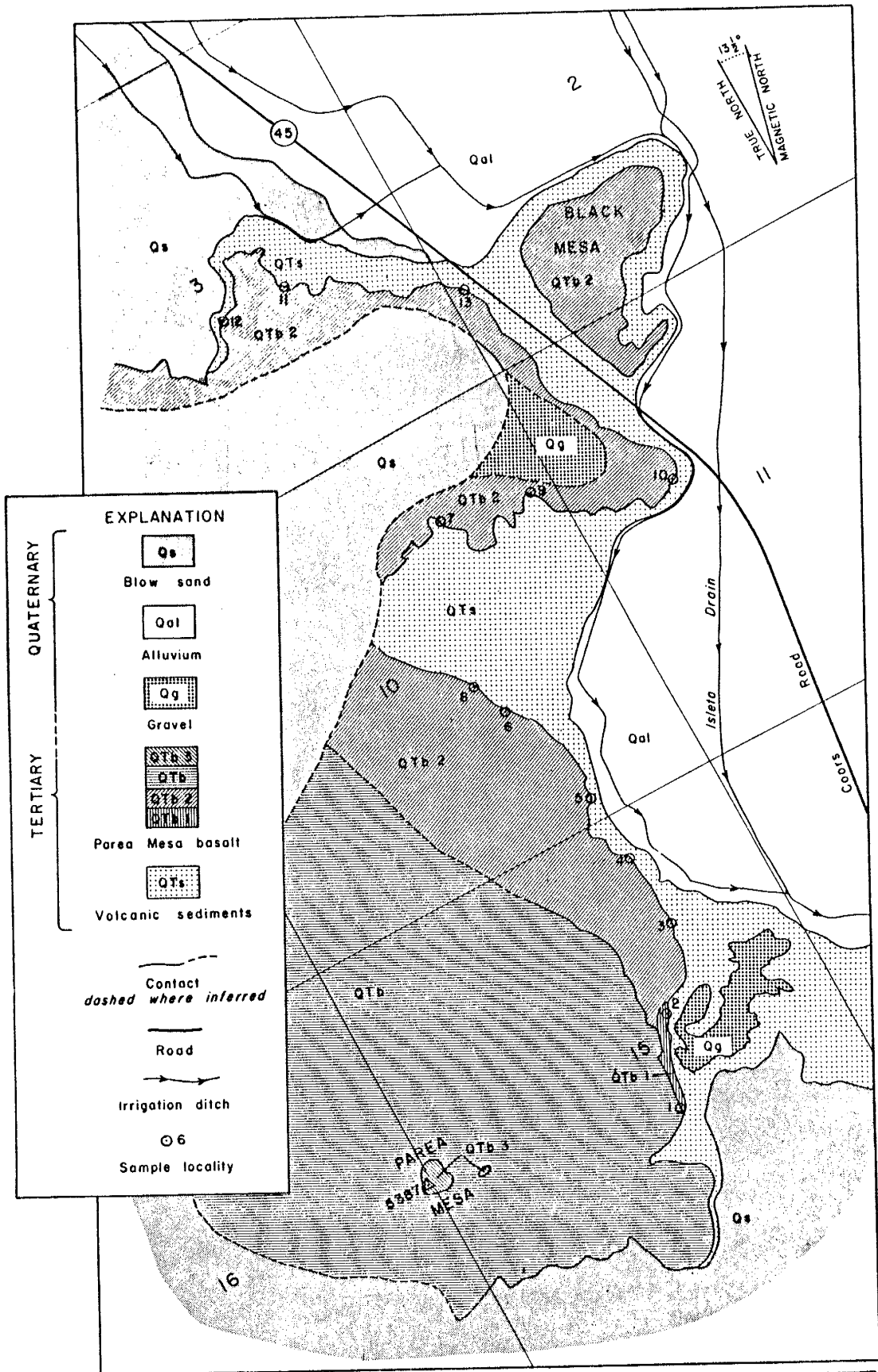
plates 1-3. In every case the overlying Parea Mesa basalt is conformable with the volcanic sediments.

The volcanic sediment is composed of thinly-bedded layers of basalt fragments with varying proportions of quartz sand and silt; the material is well to very poorly sorted and fine silty layers alternate with predominately sandy and gravelly layers. Calcite cement is common throughout. Within certain layered sequences, boulders crop out along the same stratigraphic horizon at intervals of from 3 to 20 feet. In every case a local thinning occurs in the bedded sediments. In spite of the thinning, the bedding lithology appears to be continuous both below and above the boulders. The distortion of layers is apparently due to compaction. A thickness of about 50 feet is measurable, but the base of the volcanic sediments is not exposed in the field area.

Directly overlying the volcanic sediments are the various flows of the Parea Mesa basalt. The Parea Mesa basalt is probably made up of many flows and flow-units (?). Four flows have been shown in figure 1. Flows are distinguished from flow-units, as defined by Nichols (1936), by the fact that successive flows usually are separated by a longer time interval which may be indicated by non-basaltic deposition. Flow units, as described by Nichols, are absent in the sampling area, and flows have been observed to be laterally continuous

FIGURE 1

Map of the Paria Mesa Basalt.

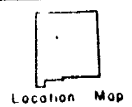
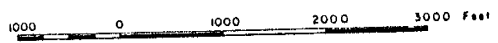


EXPLANATION

QUATERNARY		Blow sand	
		Alluvium	
		Gravel	
	TERTIARY		Volcanic sediments
			Parea Mesa basalt
			Volcanic sediments

Contact dashed where inferred
 Road
 Irrigation ditch
 Sample locality

Base: ISLETA, N. MEX.
 N 3452.5 - W 10637.5 / 7.5
 1952



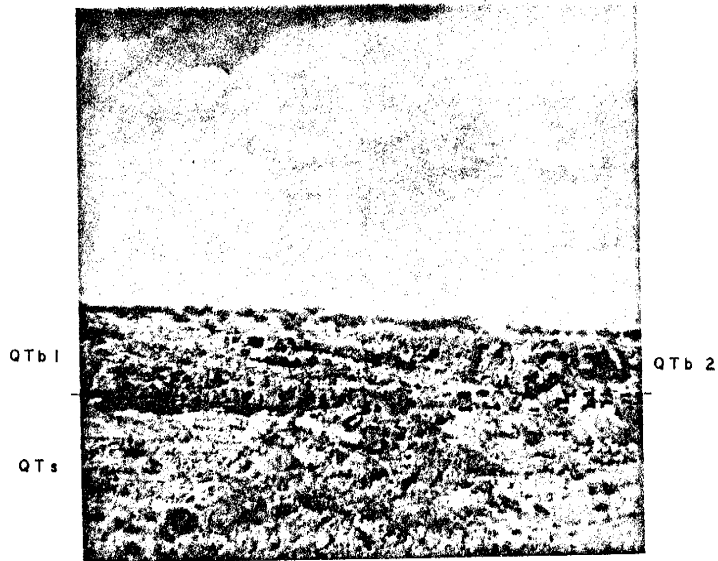
1A View northeast of sample locality number 2. looking southwest. Note upper flow units which define the edge of QTb, the north-westerly dip of QTs (upper unit only) and the gravel pediment of Qg in the foreground. Note the outcrop of the lowermost flow of QTb at the top, and QTb₁ below. Also note the veneer of gravel (Qg) which forms an angular unconformity with the northwesterly dipping volcanic sediments (QTs-2).

1. SUMMARY

1B View approximately 300 feet north of sample locality number 2 looking west, where QTb₁ and QTb₂ overlap along the outcrop. Notice that flow QTb₁ is continuous to a very thin edge. The total thickness of both flows is between 6 and 7 feet. The deposit between flows is a very thin silty zone, less than a foot in thickness. View of QTs is perpendicular to the strike and the dip is 15° NW.



A



B

to less than 6 inches in thickness (plate 1B). This indicates a high fluidity and it may be that the flow-unit mechanism of movement, described by Nichols (1936), was not active in the Parca Mesa flows.

At sample locality 1 two flows are present. The lower flow is 20 feet thick, and the upper flow is approximately 10 feet thick. The lower and upper flows are separated by a thin silty horizon, 1 to 2 feet in thickness. Both flows are continuous and have about the same thicknesses to sample locality 2 (plate 1A). About three hundred feet northeast of sample locality 2 (plate 1B) the lower flow (QTb₁) pinches out and a new flow (QTb₂) overlaps it. The lower flow QTb is not coextensive with either flows QTb₁ or QTb₂, as shown in figure 1 and plate 1A. Plates 1 and 3 illustrate typical exposures of QTb₂ and the conformable contact between QTb₂ and the underlying volcanic sediments, QTs (Plate 2A).

An unusual feature of QTb₂ is the occurrence of spheroidal zones. These zones range from 6 inches to 4 feet in outcrop diameter, see plates 2A and 2B, and appear to be localities of intense alteration; possibly indicating autolithic assimilation and/or reaction. These spheroidal zones do not appear to be pillow structures, nor were any other features commonly ascribed to aqueous chilling (Russel, 1902; Fuller, 1931) observed in the field area of the Parca Mesa basalt. That is, although the bottom portion of QTb₂ is very vesicular and, in places,

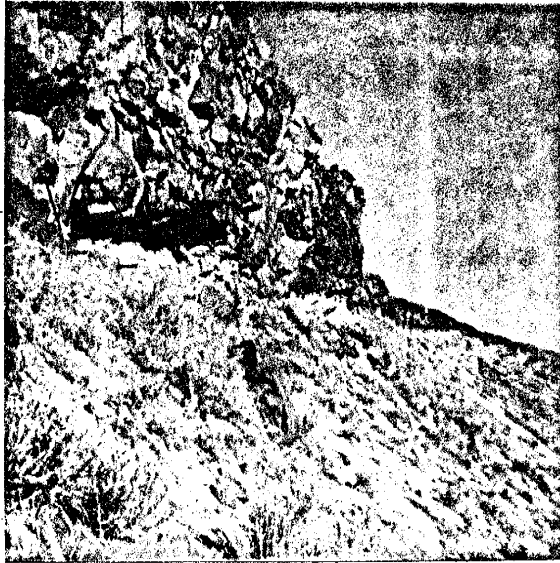
2A View several hundred feet southeast of sample locality 6 looking northwest, illustrating the decrease in thickness of QTb₂ along the western limb of the Parea Mesa basin. The thickness of QTb₂ in the foreground is 30 feet while that in the background is 5 feet. Arrows denote spheroidal zones. Note the basinward dip illustrated by the exposed portion of the flow bottom.

S. BEALIN

2B View near sample locality 11 looking south. Note the large, central spheroidal zone which is sharply outlined by weathering. The contrast in color and surface texture between the spheroidal zone and the lighter gray basaltic material adjacent to vertical joints, and in the lower and upper parts of the flow are clearly defined. The thin bedding in the underlying QTs dips gently eastward. The hammer handle is 10 inches in length.

QTb 2

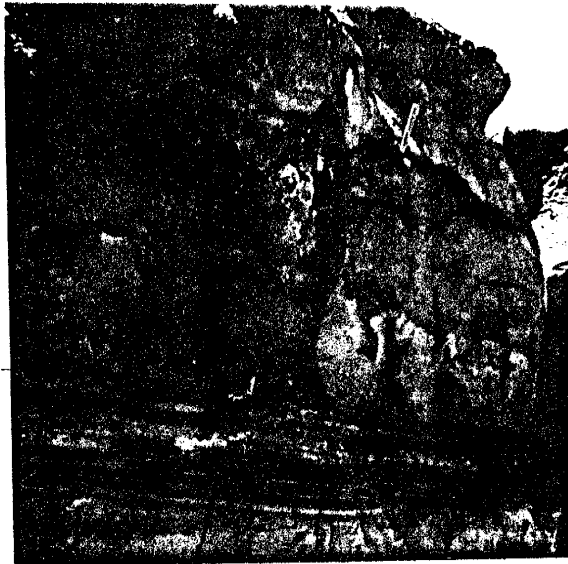
QTs
&
Qs



A

QTb 2

QTs

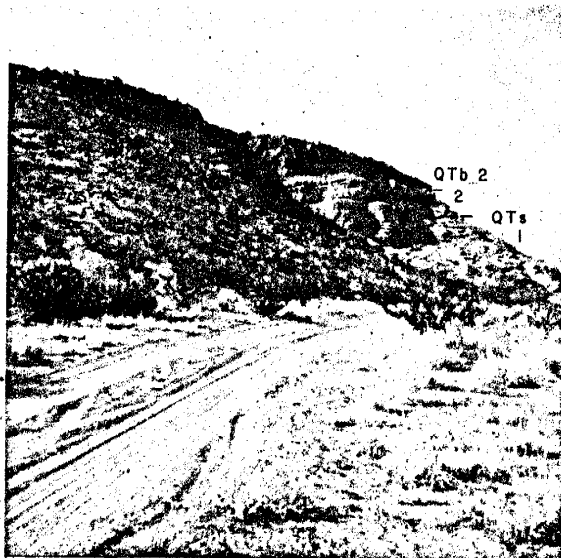


B

3A View looking north toward sample locality 5 looking northeast, illustrating the truncation of the gentle easterly dipping QTs-1 by the steeper westerly dipping beds of QTs-2. Note the increase in basalt thickness in the westward re-entrant into the northern portion of the Parea Mesa basin.

PLATE 3

3B View southeast of sample locality 6 looking southwest, illustrating the thickest outcrop of QTb₂ which denotes the cross-section of the axial portion of the northern portion of the Parea Mesa basin. The thickness there is approximately 40 feet and the basinward dip is 28° to the southwest.



A



B

quite rubbly (plate 3B), in hand-specimen the groundmass is not vitreous. In addition, the spheroidal zones occur in the top, bottom or central portions of QTb₂, these latter two occurrences are pictured in plates 2A and 2B.

The upper flows of QTb are not mapped as separate units because their relationships are concealed by basaltic talus; the approximate distribution of these flows is indicated by the outer margin of the lowest flow of QTb, plate 1A.

A much later flow on the top of Parea Mesa, designated QTb₃, is about 10 feet thick and probably represents the last eruptive phase of volcanic activity in the area.

Parea Mesa is roughly conical in shape, but has no recognizable central vent or crater. Local patches of reddish (oxidized?) scoriaceous material, suggesting explosive activity and possibly a local cinder cone or vent, but the continuity of this feature is obscured by the final eruptive phases and the talus covered slopes.

Gravel (Qg) 1 to 10 feet in thickness, consisting predominately of granite, gneiss and quartzite pebbles, is found in two localities in the Parea Mesa field area (figure 1). These gravels overlie QTb₂ in the northern portion of the field area and the volcanic sediments (plate 1A) and a thin unmapped basalt outlier in the southern portion. In the

northern portion these gravels are 120 feet above the present Rio Grande flood plain, while in the southern portion they are approximately 100 feet above the Rio Grande flood plain. It is thought that these gravels cover remnants of a former pediment surface, left after partial exhuming of the area, and are probably equivalent in age to the Segundo Alto surface of Wright (1946). Scattered pebbles of granite, gneiss and quartzite are rather common over most of the surface of the Parea Mesa basalt, thus offering additional evidence for the exhumed nature of Parea Mesa.

Alluvium (Qal) includes recent sedimentary material of the Rio Grande flood plain and basalt talus in the vicinity of the Parea Mesa.

Wind-blown sand (Qs) covers much of the mapped area, and restricts the exposure of the Parea Mesa basalt to the south and southwest. The wind-blown sand represents an active eastwardly advancing front of fine sand which prevents the tracing of flow QTb₂ between sample localities 7 and 8. However, QTb₂ is believed to be continuous under the sand cover, because of its inferred high fluidity and the lack of a co-extensive development of immediately adjacent flows of stratigraphically higher or lower flows.

STRUCTURE

The structural evolution of the Parea Mesa area is beyond the scope of this paper, insofar as the author's problem is concerned. However, some of the problems concerning the structural evolution include: the study of water-laid versus or including aeolian agents of transport and deposition for the volcanic sediments; the unusual character of the volcanic sediments, including the boulder layers and large-scale truncation; and the relationship of the Parea Mesa basalt flows to the pre-flow surface of the volcanic sediments. These last two features are of interest since the thickness and distribution of the Parea Mesa basalt seem to be a function of its structural relationship of the underlying volcanic sediments.

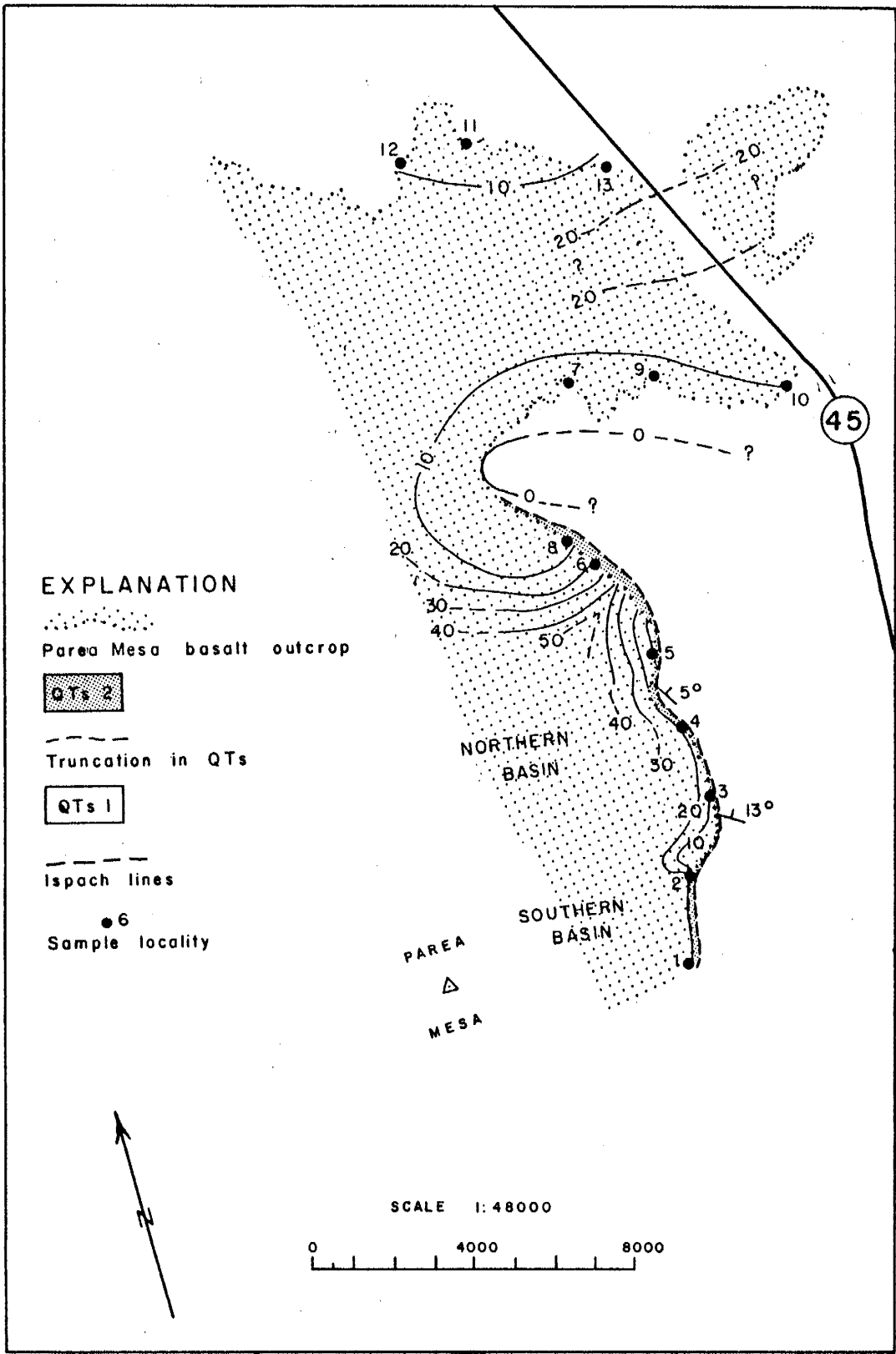
In the northern part of the Parea Mesa area the volcanic sediments have nearly a horizontal to a gentle eastwardly structural attitude, denoted by QTs-1, with local irregular dips of 0 to 6 degrees. The pre-flow surface formed by these beds is parallel to this structural attitude (plate 2B) and on the basis of QTb₂ outcrop thickness it is inferred to be of low topographic relief. Volcanic sediments of this same structural attitude are found in the southern portion of the Parea Mesa area, except that there these beds are truncated in their upper portion by beds of similar lithology (plate 3A). The truncating beds

are found only in the southern portion of the Parea Mesa area and represent a second, westerly, structural attitude, denoted by QTs-2. Minor faulting in the beds of QTs-1 in the vicinity of this angular unconformity appears to be associated with the tectonic activity which gave rise to this truncation; faulting was definitely pre-QTb₂.

The volcanic sediments of the second structural attitude have westerly dips of 15 to 30 degrees (plates 1A, 2A, 3A, and 3B). The attitudes of these beds indicate that the pre-flow surface of the southern portion of the Parea Mesa area was an elongate asymmetrical depression or basin whose axis is southwest-northeast. This depression called the Parea Mesa basin is composed of northern and southern parts, and is believed to be a product of pre-flow subsidence. Flow QTb₁ is believed to have been largely restricted to the southern portion of the Parea Mesa basin and flow QTb₂ is generally restricted to the northern portion. The evidence for these postulated relationships includes: the fact that only one flow (QTb₂) exists north of the approximate dividing line within the basin (plate 1B and figures 1 and 2); the fact that QTb₂ is everywhere conformable with QTs-2 (plates 2B, 3A and 3B); and the inference that outcrops near sample localities 6 and 8 transect the axis of the northern portion of the Parea Mesa basin (plates 3A and 3B). The character of the pre-flow surface of QTs-1 and QTs-2 is indicated in figure 2, in which it is assumed that the

FIGURE 2

Isopach map of flows QTb₁ and QTb₂ which have essentially horizontal upper surfaces, thereby illustrating the pre-flow, structurally controlled, surface of QTs. The Parea Mesa basin framed by QTs-2 has been subdivided into southern and northern parts, and is believed to be the result of pre-flow subsidence.



upper surface of the basalt is horizontal. This figure illustrates the author's hypothesis that the distribution and thickness of QTb₁ and QTb₂ is controlled by the structural attitudes of the underlying volcanic sediments.

The gross lithology and structure of the volcanic sediments of the Parea Mesa area bear a marked resemblance to the volcanic sediments related to diatremes of the Hopi Buttes area, Arizona; Williams (1936), Hack (1942), and Shoemaker (1956). The term diatreme has been used to denote the structural and lithologic features associated with volcanic vents of an explosive nature. Shoemaker (1956) has noted that the difference between diatremes is related to the amount of subsidence and extent to which each vent and its associated sediments are exposed. That is, in the proximity of the vent there is periodic explosive volcanic activity associated with pre- or post-volcanic subsidence, and during periods of quiescence there is aqueous or nonaqueous sedimentary deposition. Therefore, as a gradual and progressive subsidence takes place the depression is filled with sediments, chiefly of volcanic origin, in which angular unconformities are common. Shoemaker (1956) has also noted that the structural depressions formed by diatreme tectonics probably become the locus of lava extrusion after collapse has ceased. Thus,

the author has concluded that the general structural features of the volcanic sediments of the Parea Mesa area are best explained by diatreme-like tectonics.

SAMPLING

The Parea Mesa basalt was sampled in 13 localities as shown on figure 1, and a total of 57 samples were collected. The sampling interval was approximately 1,000 feet. Field studies have revealed that the first two sample localities were confined to QTb₁ and QTb, while the remaining sampling localities are believed to be solely from QTb₂.

At each sample locality a minimum of four samples were obtained. One sample was a composite, composed of chips taken at 6 inch intervals from the bottom to the top of the flow. The second, third, and fourth samples were grab samples broken from the outcrop: one foot from the bottom; in the approximate middle; and within one foot of the top of the flow outcrop. Each grab sample weighed approximately 2 pounds, while the composite samples were on the order of 3 pounds each. At sample localities 6, 10, 11, and 13 spheroidal areas in the outcrop (see plate 2) were also sampled in addition to the four regular samples. The samples were labeled with a number which denoted the sample locality and the chip composite and a letter to indicate the grab position within the sample locality (e. g. 6S-spheroidal zone, 6T-top, 6M-middle, 6B-bottom, 6VB-very bottom, and 6-composite chip).

The reasons for the different types of samples described above are twofold. First, a check between the data obtained from the composite chip sample and the grab samples furnishes information concerning variation with respect to sample position. Secondly, inasmuch as composite chip samples are difficult to obtain in most field occurrences of basalt, the comparison of composite chip samples with grab samples might yield information concerning the reliability of samples collected from the top surfaces of a flow as compared to samples taken at the bottom or middle of the flow. The composite chip sample is assumed to be the most representative sample at any given locality because any vertical variations which might exist have been integrated. Bottom, middle, and top grab samples also furnish information concerning variations in these horizons, and the averages for all samples from a given horizon can be compared.

LABORATORY STUDY

The laboratory work involved detailed study of all grab samples, supplemented with thin-section analysis of grab samples from a few selected localities, and x-ray determination of the composition of phenocryst olivine. Variations with regard to sample position and locality have been noted, and statistical analysis is applied to observed variations in olivine composition.

Hand Specimen Study

All grab samples were examined to determine: gross structure; percent and shape of vesicles; the nature of vesicle filling material; color of fresh and weathered surface; the mineralogy, shape, size and color of phenocrysts; and color and extent of alteration. No gross differences were observed between the thin-sections and grab samples from QTb₁, QTb₂ or QTb. However, similarities were observed in QTb₂ between grab samples of the same relative vertical position; rock color and structure vary with sample position.

In hand specimen the fresh surface color can be used as a general indication of vertical sample position for any sampled locality. In general, samples from the bottom of the flow are

black to dark gray; samples from the middle and within approximately 3-4 feet of the top and base of the flow are dark bluish to greenish-gray (particularly those samples from spheroidal zones); and samples from the top of the flow and along joints in the flow (i. e. 3 to 10 inches on either side) are light gray to light brownish gray. The divergence in color is principally the result of alteration and/or contamination. The color of the uppermost grab samples is essentially that of unaltered basaltic material. The color shown in the central and spheroidal zones is due to the green alteration products which change outwardly into red alteration products; in turn the red alterations products diminish toward joints and toward the top (plate 4). The color of bottom samples appear to be more affected by contamination; alteration and/or weathering products are black, green and red.

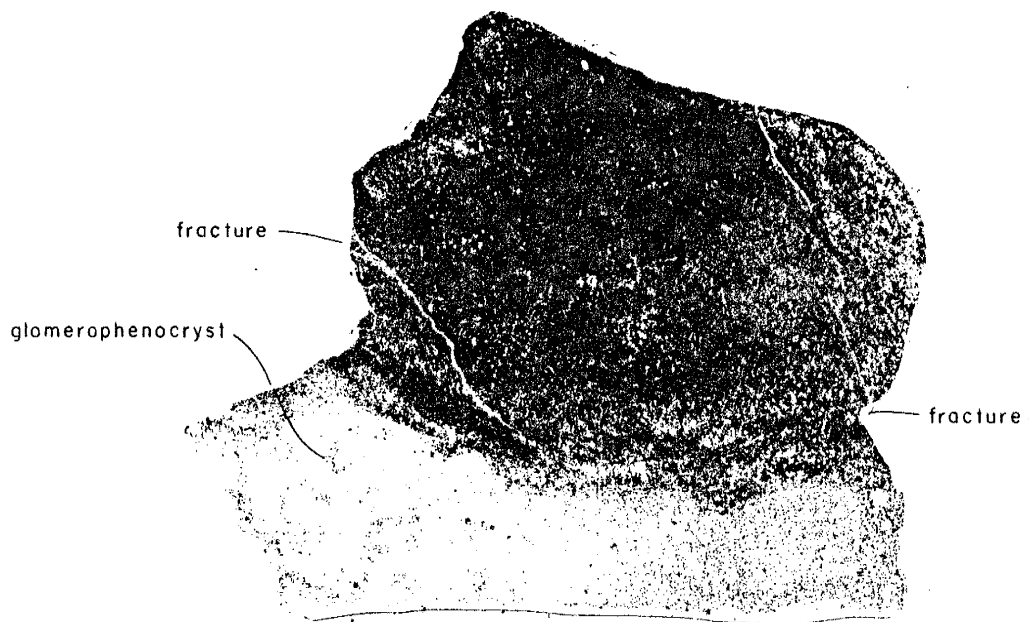
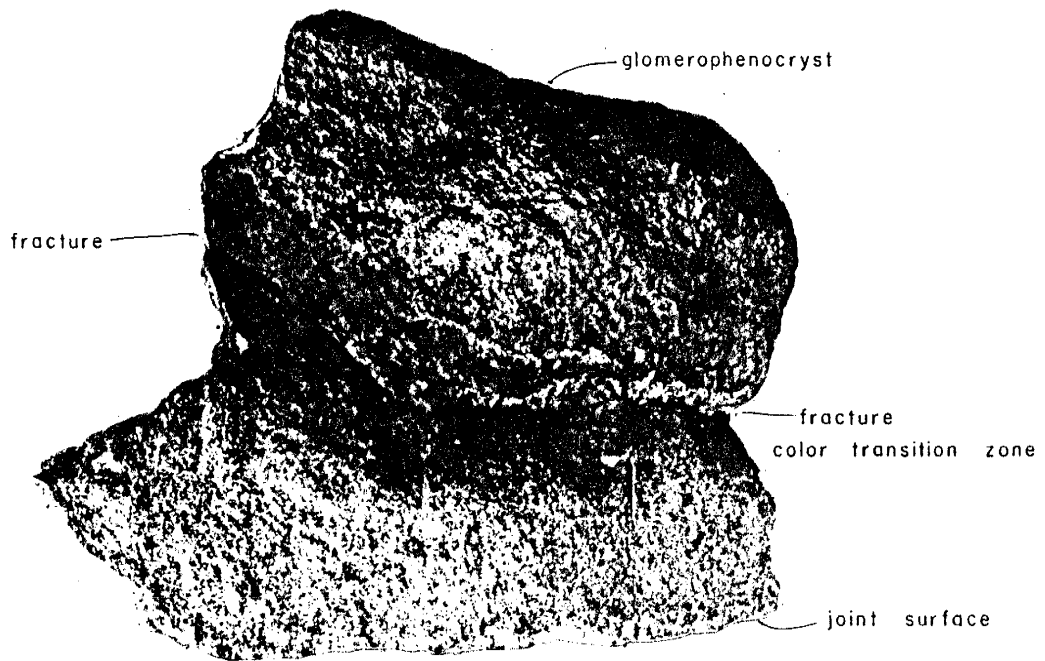
The structure of the grab samples varies systematically with position in the flow. The bottom samples are quite vesicular in a zone which extends upward for 6 inches to 2 feet from the base of the flow, before grading into a more massive middle portion. The massive middle portion grades in turn into a vesicular upper portion.

Vesicles near the bottom are irregular in outline but generally are flat, with their longest dimension (0.5 to 3 inches) parallel to the pre-flow surface. Some samples, collected at the very bottom of the flow, are bright orangish red, as are the edges and interiors

4A Hand specimen showing rounded surface of spheroidal zone which is separated from an outer lighter gray area by a fracture. Note that fracture bears very little relation to the change in color, denoted here by a change in contrast. The lower margin appears to be a joint. A glomerophenocryst is shown in the upper-central portion.

DETAILS

4B Sawed and ground surface of the same sample. Note that the fracture bears very little relation to the change in contrast. Mottled appearance of the lighter material adjacent to the joint fracture is due to irregular distribution of red alteration products.



of most of the vesicles near the base. The vesicle filling material is commonly calcite. Vesicles constitute between 10 and 50 percent of the volume of the flow, with the average being approximately 30 percent.

22567

The gross structure of the middle portion of the flow is massive and nonporous with only 2 to 3 percent of the volume as vesicles. Many sample areas in the middle portion of the flow show changes in color, particularly along joints. These color differences are intensified where spheroidal areas (see plates 2 and 4) are exposed by surface spalling along fractures but may be quite irregular. Plate 4B illustrates the color contrast between a spheroidal area and an outer shell on a sawed surface, while plate 2A illustrates the color differences on the weathered surface. Although the spheroidal shape is outlined by a fracture on the weathered surface, the color change is gradational on the cut surface and not necessarily related to fractures. The spheroidal zones are quite resistant to weathering. Amygdules from the middle portion of the flow are spherical and from 0.1 to 0.3 inches in diameter. The amygdaloidal material is transparent to earthy. The transparent material is calcite. The earthy material is from brown to olive green to pea green in color and is particularly restricted to spheroidal areas. Optical study utilizing immersion oils reveals the range in indices of 1.54 to 1.51 for light-green, fine-grained aggregates and fibrous rosette-like clusters which are length

slow. Qualitative x-ray fluorescent analysis indicates the presence of iron. X-ray diffraction analysis yields an expanded basal reflection of 17.8 - 17.9 Å, with an integral series of higher order basal reflections. It has been concluded that this material is an iron rich montmorillonite.

The upper portion of the flow contains from 1 to 40 percent vesicles and has a more porous groundmass than the middle and bottom parts. The vesicles range in size from 0.5 to 3.0 inches and are circular to elliptical in cross-section, usually with smooth inner surfaces; some clear to milky calcite amygdules are present in minor amounts.

Thin-Section Analysis

Thin-sections were made of the grab samples obtained from sample localities 1, 6, 8 and 13. The top grab sample from locality 1 was from QTb, the middle and bottom samples were from QTb₁, and all the rest of the grab samples of which thin-sections were made were from QTb₂. The Parea Mesa flows, QTb, QTb₁ and QTb₂ are porphyritic to glomeroporphyritic olivine basalts with similar mineralogy. Calcic plagioclase, olivine and pigeonite are the principle phenocrysts and together comprise 10 to 15 percent of the rock mode (see table 1). Glomerophenocrysts have intersertal to subophitic textures; a minor amount of fibrous zeolite, thomsonite,

was found in the interstices of some glomerophenocrysts. As a rule olivine and calcic plagioclase occur together, while olivine and pigeonite are more common as monomineralic aggregates.

Individual phenocrysts of calcic plagioclase within the groundmass are subhedral, usually having angular terminations. The composition of phenocryst plagioclase is bytownite with a range of An₇₁₋₇₃. The composition bytownite was based on Michel-Levy's method, utilizing the maximum extinction angle of albite twins, in conjunction with Tsuboi's method using the maximum index of the (010) cleavage (Rodgers and Kerr, 1942). Bytownite crystals are commonly zoned and show recrystallization of corroded areas. As many as twenty zones were observed on a single crystal and, as a rule, the cores are more calcic than the borders, while intermediate areas exhibit alternating zones of intermediate composition. The composition of groundmass plagioclase feldspar is An₅₄₋₆₅ (i. e. labradorite) using the method of Michel-Levy. Labradorite laths form the groundmass network (see plate 5).

Olivine crystals are euhedral to subhedral in aggregate occurrences with bytownite, but are subhedral to angular as individual phenocrysts. It is not known whether all individual phenocrysts of olivine are related to the aggregate occurrences, but it is thought that the angular phenocrysts of bytownite are clastic

TABLE 1. Modal Analysis for the Parea Mesa Basalt¹

Mineral	Volume % range	Size in mm.
Phenocryst fraction	10-15	-
Bytownite An ₇₁₋₇₃	3-8	1-3
Olivine	4-10	0.5-1.5
Plagioclase	0.5-1	0.5-1
Groundmass	85-90	-
Labradorite An ₆₄₋₆₅	50-60	0.05-1.30
Olivine	10-20	0.05-0.2
Diopside	10-20	0.05-0.2
Magnetite and/or Ilmenite	5-10	0.05-0.1
Apatite	Trace	0.05
Zircon	Trace	0.05

¹ Mode does not include alteration products.

fragments of these and a moderate portion of the individual olivine phenocrysts may have been derived in a similar manner. The general features of these glomerophenocrysts indicates that they are autoliths inclusions of genetically related rock which may have crystallized in

an intratelluric environment. Zoning is apparent in some olivine crystals and is outlined by layers of magnetite dust or internal iddingsite alteration (plate 5). Most olivine phenocrysts include opaque blebs or cubes of unidentified iron or iron-titanium oxides. Embayments of olivine phenocrysts are present but are not ubiquitous, while pyroxene coronas or reaction rims are absent. The olivine phenocrysts have a 2V so close to 90 degrees that the optic sign is apparently neutral. Groundmass olivine is clear under plain polarized light and occurs as intergranular anhedral crystals in the labradorite groundmass network (see plate 5). These small olivine crystals show slight to complete iddingsite alteration.

Pigeonite is the least common of the phenocryst constituents and is usually euhedral in individual phenocrysts and subhedral in aggregates. Zoning, twinning and recrystallized areas are common in pigeonite crystals. Both polysynthetic twinning on (001) and twinning seams on (010) were observed. Pigeonite may be distinguished from groundmass diallage mainly by better developed cleavage, 2V of 15-20°, and maximum extinction on (010) of 36°(Z \wedge c). Di-
allage has poorly developed cleavage, 2V of 30-40° and Z \wedge c maximum extinction on (010) of 48°. The color of phenocryst pigeonite is pale gray in basal sections and colorless in other orientations. Di-
allage is confined almost exclusively to the groundmass while pigeonite has not been identified in the groundmass. Groundmass diallage is

5A Photomicrograph, plane-polarized light, showing an aggregate occurrence of olivine phenocrysts (O), and a relatively unaltered groundmass of labradorite (L), diaspore (D), magnetite (M), and olivine (O). Note that iddingsite (I) alteration is, in some cases, within the crystal boundaries of olivine. The general unaltered nature of the groundmass is characteristic of the upper portion of flow QTb₂. 3 31214

5B Same as above with nicols crossed.



A

1.0 mm



B

1.0 mm

colorless to pale gray and is unaltered except in the groundmass near the bottom of the flow. Diagenesis is generally intergranular in the network of groundmass labradorite (see plate 5).

Alteration and groundmass texture of the Parea Mesa basalt vary depending upon sample position in the flow, and are found to be generally consistent between sample localities. Alteration present in the basal part of the flow is distinctly different from that found in the middle and upper portions. The groundmass is essentially opaque yielding a hyalo-ophitic texture in which the original groundmass constituents can only be inferred in areas where vague differences in birefringence can be seen. This altered groundmass is composed predominantly of dense opaque crystallites which illustrate margarite and cumulite forms near the borders of plagioclase and olivine phenocrysts. Olivine phenocrysts have opaque alteration along fractures as well as along linear extensions away from fractures which are parallel to subparallel to crystallographic directions. Other alteration products of olivine include red iddingsite and a green alteration product believed to be smectite-chlorite, Wilshire (1958); both are similar in occurrence to that of the opaque material. The groundmass constituents (plagioclase, pyroxene and olivine) are almost completely altered in the basal portions but become readily recognizable within 3 inches to a foot of the base, as the density of opaque crystallites decreases. Presumably this type of alteration is

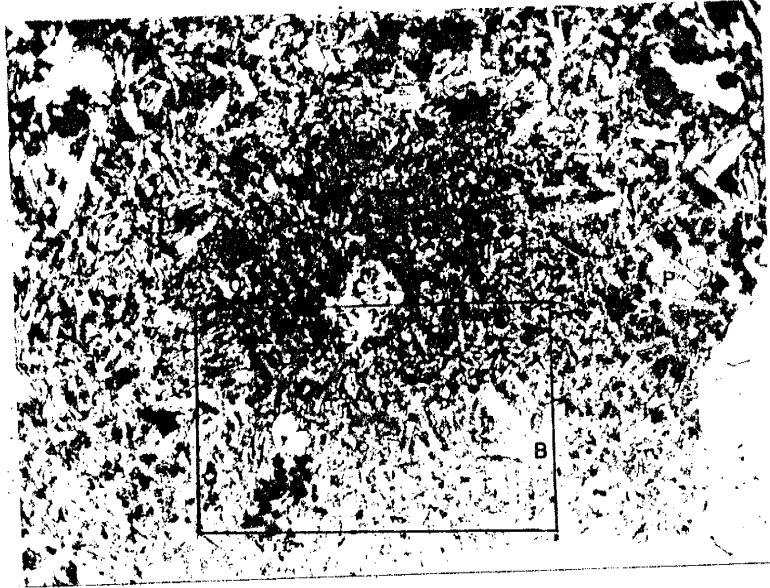
due to contamination by solids and volatiles from the underlying sediments which may have had a combined effect with deuteric solutions.

Amygdules in the bottom part of the flow are filled predominantly with coarsely crystalline calcite. An isotropic black to orange material, chlorophaeite (Peacock and Fuller, 1928), is also present. Chlorophaeite also occurs in a few groundmass interstices, where it usually is associated with an anisotropic material of similar color that is fibrous (length-slow) to microcrystalline, and which may be iddingsite or smectite-chlorite, Wilshire (1958).

Alteration of the central portion of the flow is the most intense of any of the areas examined with the exception of spheroidal zones. Both spheroidal zones and the central portions of the flow exhibit similar type alteration in which the gross color of the alteration product is green. Within the spheroidal zones there are loci of intense alteration which have cores of very pale green to clear fine-grained aggregates (probably montmorillonite on the basis of its amygdaloidal occurrence) which grade outward into dark green, olive green and light green alteration products (plate 6). Dark green alteration products are massive with only vague extinctions and commonly form pseudomorphs after olivine, plagioclase, and pyroxene phenocrysts (plates 6 and 7). Pseudomorph extinction, if present, is generally in the direction of the relict host mineral cleavage.

6A Photomicrograph, plane-polarized light, showing the intense alteration characteristic of spheroidal zones. The change in contrast of the alteration products illustrates an approximate zoning with; the darkest being located close to the center and forming pseudomorphs after olivine (PO), lighter also forming pseudomorphs after olivine (PO), and groundmass plagioclase (PP); and the lightest which is restricted to groundmass interstices. Mineral constituents include bytownite (B), labradorite (L), magnetite (M), diaspore (D), clay (?) (C).

6B Enlargement of outlined area in 6A.



A

1.0 mm

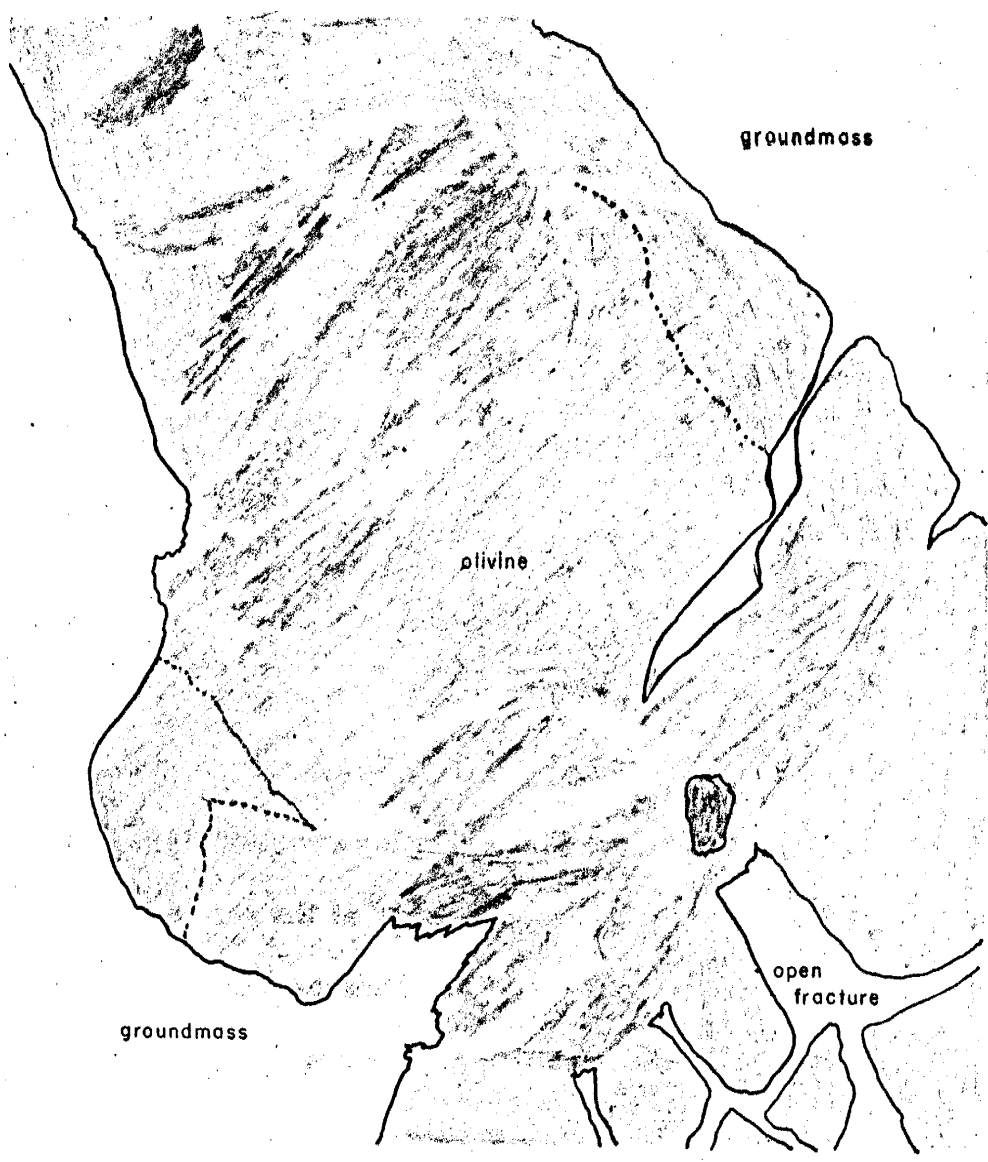


B

1.0 mm

PLATE 17

Photomicrograph of pseudomorphic alteration product of olivine using vertical illumination. Note the definite fibrous habit and banded texture of the alteration product. The accompanying overlay furnishes an idea of the variation in color of the bands which are actually an end-on view of micaceous plates in brown and amber areas. Green areas are composed of a very massive fine grained to fibrous material.



groundmass

olivine

groundmass

open
fracture



0.1 mm



—
0.1 mm

Olive green alteration products form pseudomorphs after olivine and plagioclase phenocrysts and fill interstices of groundmass plagioclase. Olive green alteration products differ from the dark green alteration products in color, occurrence, and crystallinity; they are microcrystalline to fibrous, length-slow. The light green alteration product is also microcrystalline to fibrous (length-slow) but only occurs in the interstices of groundmass plagioclase.

Plate 7 illustrates a pseudomorph of green alteration after olivine, as viewed by vertical illumination. The nature of the color banding is illustrated on an overlay. The view is approximately parallel to the micaceous cleavage of the dark brown and greenish brown pseudomorph material. The light to yellowish green material is finer grained and massive. Microscopic examination utilizing immersion oils indicates that the color varieties of the green alteration product have indices which lie within the range of 1.57 to 1.54. Here the variation in crystallinity is more apparent; the massive green material is composed of microcrystalline aggregates which are oriented in such a way as to impart gross optical properties to the fragments. The cleavage of this variety is imperfect, parallel to the slow direction. The dark brown and greenish brown materials of plate 7 were observed as plates in the loose grain study. These plates were optically negative with a $2V$ less than 5 degrees. On several such plates N_p and N_y were equal to 1.564 ± 0.002 . Both the micaceous and the

massive materials were analyzed using x-ray diffraction and both yielded four measurable reflections: a broad but intense reflection at 14 Å; and less intense reflections at 4.6 Å, 2.65 Å and 1.52 Å. Undifferentiated pseudomorph material was then treated with ethylene glycol and x-ray analysis revealed broad reflections at 16 Å and less intense reflections at 9 Å, 8.5 Å, 7.2 Å and 4.4 Å. The character of the reflections from the glycolated material was poor and those spacings given represent the most frequent reflections from more than ten x-ray runs on the same material using both Ni-filtered Cu radiation and Mn-filtered Fe radiation. X-ray analysis of this same material after 24 hours heating at 700°C yielded a broad reflection between 10.8 and 9.5 Å with a poorly defined plateau at approximately 14 Å. It has been concluded that the green alteration products of spheroidal zones and central portion of OTb_2 are composed of montmorillonite and an expandable vermiculite, plus a minor amount of chlorite. The distinction between montmorillonite and vermiculite is one of grain size; vermiculite is coarser (Weaver, 1956). Chlorite is indicated by the lack of a full 17 Å expansion with ethylene glycol, nonintegral higher order reflections of the basal spacing for the glycolated material and the plateau at 14 Å on the heated material. Wilshire (1958) has used the term smectite-chlorite to describe material of similar nature from extrusive rocks. This same terminology will be used by the author in view of the fact

that chlorite may occur as an independent phase or as an inter-layered constituent of montmorillonite and vermiculite (i. e. smectite). Montmorillonite of earthy amygdules of spheroidal zones differs from these green alteration products by its finer grain size and 17.8 Å basal spacing with glycolation with an integral series of higher order basal reflections. Further detail as to the exact mechanics of alteration and the chemical changes involved are beyond the scope of this paper.

Another feature of the green alteration products is their color transitions into reddish alteration products which are similar in crystallinity and occurrence. This transition (plate 4) appears to be a secondary product after the green varieties and is usually present in a rather narrow zone between altered spheroidal areas and unaltered outer areas. Both products occur as alteration products of olivine and plagioclase, and fill interstices in the groundmass (see plate 8). Although the explanation and origin of these alteration products is beyond the scope of this study it is important that the studies of Wilshire (1958) and Brown and Stephen (1959) indicate that layered silicates, montmorillonite, vermiculite, smectite and chlorite may alter to the goethite, the pigment and major mineral constituent of iddingsite, with a possible end product of goethite and of amorphous silicates (Sun, 1957). Both red and green alteration products have a similar mode of occurrence in olivine phenocrysts (plate 7); forming

first along fractures and crystal borders, then showing linear extensions into the host which are in alignment with the optic and crystallographic elements of olivine (plate 5). Plates 6 and 8 illustrate the other occurrences of the red and green alteration products in more intensely altered areas.

Alteration minerals found in the upper portion of the flow consist solely of calcite and iddingsite. Calcite occurs after plagioclase and fills interstices, while iddingsite is restricted mostly to olivine. An interstitial occurrence of iddingsite gives a mottled appearance to the gross color in some instances (plate 4). In this occurrence iddingsite is fibrous to microcrystalline, but the color and high birefringence make further optical properties rather indeterminate. This occurrence and the occurrence after olivine are similar to the earlier description of red and green alteration products.

The time and nature of alteration which has yielded this complex aggregation of alteration products is thought to be late stage deuteric solutions with minor subsequent changes due to weathering.

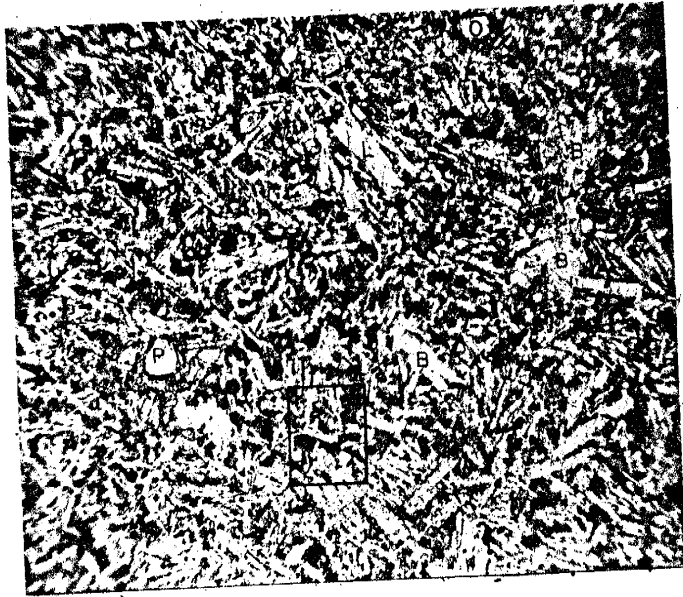
8A Photomicrograph, plane-polarized light, showing the distribution and occurrence of red alteration products characteristic of central and border portions of spheroidal zones. Minerals include bytownite (B), labradorite (L), olivine (O), pigeonite (P), diopside (D), magnetite (Mt) and red alteration product (RA).

8B Enlargement of outlined area in 8A.

8 (ETA) 10

8C Photomicrograph, plane-polarized light, showing the distribution and occurrence of the green alteration product (GA). Mineral constituents labeled as above. Notice the similarity in distribution and occurrence as shown in plates 7A and 7B.

8D Enlargement of outlined area in 8C, notice the occurrence of alteration about olivine and the occurrence in the fractures of groundmass labradorite.



A

1.0 mm



B

0.1mm



C

1.0 mm



D

0.1mm

X-ray Investigation of the Olivine

Phenocryst Fraction

Bowen (1928) noted that olivine is one of the first minerals to crystallize in natural silicate melts. Inasmuch as the olivine phenocrysts in olivine basalts and related rocks are believed to be of magmatic origin, the composition of olivine phenocrysts is thought to be sensitive to the melt composition, pressure, and temperature prior to extrusion of molten lava. The phrase "prior to extrusion" is used in light of the theoretical considerations of Bowen (1928) who inferred that olivine crystals of the phenocryst fraction were present in extrusive rocks before extrusion. Bowen's evidence is based mainly on the size of olivine phenocrysts relative to the size of the groundmass constituents and the fact that modal olivine is usually more abundant than the indicated amounts suggested by the norm or calculated olivine content.

Macdonald (1944) studied the 1840 eruption of Kilauea and attributed the difference in olivine phenocryst content, between two nearly simultaneous eruptions at different elevations, to the tapping of the upper and lower portions of the Kilauean magma column. Lavas from the lower portion of the Kilauean magma column were richer in phenocryst olivine. Macdonald concludes that olivine was more abundant because it accumulated due to gravitational

differentiation. Macdonald offers the conclusion that the olivine phenocryst fraction represents intratelluric crystallization.

The tentative findings of U. S. Geological Survey studies of the 1959 eruption of Kilauea have been reported in Science, (December 18, 1959, Anonymous).

"Early this month Murata reported that a rough correlation seems to exist between the olivine content and the temperature of the erupted material. The iron-magnesium mineral olivine apparently sinks rapidly in the magma so that a strong flushing action from deep down is required to bring it to the surface. It is during such periods of strong flow from depth that the highest temperatures can be expected."

Olivine contained in olivine basalts and related rocks is not complicated by the olivine-spinel transition at the inferred temperatures and pressures of basalt formation (Kingwood, 1958).

Naturally occurring olivine shows an isomorphous solid solution between the end-members forsterite and fayalite. The composition of olivine in this isomorphous series is mainly a function of temperature (Bowen, 1928). Sahama and Torgeson (1949) have found this isomorphous series to be thermodynamically perfect and without structural strain. Yoder and Sahama (1957) have concluded that forsterite and fayalite molecules usually make up 95 percent of most natural olivines. The remaining 5 percent in natural olivines is CaO , Cr_2O_3 , Fe_2O_3 , MnO and NiO , according to Poldervaart (1950). Tephroite, the mangan-olivine is known to

form an isomorphous solid solution series with fayalite, but is rarely found in igneous rocks, according to Rankama and Sahama (1949). The same is true of monticellite, $(Ca, Mg)_2(SiO_4)$, glaucocroite, $(Ca, Mn)_2(SiO_4)$, and larsenite, $(Pb, Zn)_2(SiO_4)$.

Although such extensive isomorphism would seem to limit the determination of olivine composition to analytical chemical methods, x-ray diffraction can furnish a rapid means by which changes in composition can be studied. Yoder and Sahama (1957) have described a method for the determination of olivine compositions which follow these specifications for atoms per formula: (p. 481)

Si: 0.97 - 1.03

X: 1.93 - 2.04

Mn: 0 - 0.03

Where X includes cations Mg, Fe, Mn etc. except Si.

Yoder and Sahama's method was used in the following investigation. Since no chemical analyses are available, the reported values are of apparent mol percent forsterite (Fo).

In preparation for x-ray analysis the entire composite chip sample, and from 1/2 to 3/4 of a pound of the grab samples from each sampling locality were crushed, pulverized and sieved. After sieving, the plus 70- and minus 149- micron size fractions were discarded, while the plus 420- and plus 149- micron fractions were retained. Utilizing a binocular microscope and tweezers, the plus 420-micron

size fraction was used in hand picking the olivine phenocrysts for subsequent x-ray analysis. Only enough olivine was picked for one mounting and as additional material was needed it was picked. Approximately 0.1 of a pound of material was processed in the selection of between 100 and 200 olivine and phenocryst fragments. It has been assumed that the errors involved in picking olivine phenocrysts from samples which have been processed in the above manner are non-systematic, as there is no method by which this could be checked; that is, the author performed all the picking. In considering possible sources of error, selective crushing of olivines of a certain composition hardly seemed possible, and since individual groundmass olivines are usually less than 200-microns, even the larger crystals of the plus 149-micron size fraction should be useable. However, it was not necessary to use this size fraction. The most important possible source of error would be that introduced by selective picking. The author was constantly aware of this possibility while picking and was more inclined to include all questionable phenocrysts and fragments rather than exclude any. Even within one grab sample the color of phenocryst olivine varied from pale green to olive green and individual crystals usually showed a reddish brown iridescence. The color can probably be regarded as a function of optical orientation relative to viewing axis, while the iridescence is believed due to iddingsite alteration. Iddingsite and

other possible mineral contaminants were of little consequence other than as diluents, since the particular olivine reflection used is widely separated from those of the possible contaminants. Contamination between samples was minimized by carefully cleaning the crusher, pulverizer and sieves between sample runs.

Other methods by which olivine reflections may be obtained include: (1) uncovered thin-sections (Yoder and Sahara, 1957); (2) finely ground bulk rock; (3) the non-magnetic fraction after magnetic separation; (4) the heavy fraction of a heavy-media separation; and (5) a combination of methods (3) and (4). Methods (2) through (5) were investigated by the author and method (2) was found to be unsatisfactory because the reflection of interest was not resolved well enough for measurement, due to mass absorption and dilutional effects of the bulk material. A combination of methods (3) and (4) yielded reflections of good resolution, but this method was not used because olivine was found in both the magnetic and non-magnetic fractions and a selective sample error was possible. Therefore, hand-picking was used in spite of the time involved in separating enough material for x-ray analysis. The average picking time per sample was about 45 minutes. Short 2 to 3 hour picking periods, separated by less tedious work, was found less tiring and more rewarding than extended periods of picking.

After each sample was picked it was re-examined for contamination, then crushed in a steel mortar and pestle and ground in an agate or porcelain mortar and pestle. In keeping with the method described by Yoder and Sahama (1957, p. 477-478) silicon powder (sieve size, minus 44-microns) was added in order that the olivine-silicon ratio was approximately three to one. The mixture was then homogenized by grinding until the color was uniform and then emptied onto a clean glass slide. A few drops of a dilute solution of lacquer in acetone were added, and the wet sample was stirred with a small spatula to a thin film covering the known x-ray target area on the glass slide. The mounted samples were exposed to Ni-filtered Cu radiation, with a Norelco high-angle x-ray diffractometer. Records were made at 1 inch per degree 2θ . The divergent and scatter slits were 1° , receiving slit 0.003 inch, and the scan speed was $1/4^\circ 2\theta$ per minute. The x-ray apparatus was set to oscillate between 28° and $33^\circ (2\theta)$ and for every sample at least four oscillations (two up- 2θ and two down- 2θ) were measured for any one composition determination. The position of the olivine (130) reflection was obtained by first measuring the distance between the olivine (130) reflection and the silicon (111) reflection. This distance was then added to the value of the silicon (111) reflection given by Phillips Laboratories, 28.440° for $\text{CuK}\alpha_1$. The corrected 2θ value for the olivine (130) was then converted to the Bragg's equation equivalent in Angstrom units,

using conversion tables by the National Bureau of Standards. The interplanar spacing $d(130)$ was obtained to five places. The mol percent forsterite (Fo) was then calculated using the formula of Yoder and Sahama (1957, p. 485).

$$\text{Fo(mol\%)} = 4233.91 - 1494.59 \cdot d(130)$$

(shown in figure 3)

where mol percent is the notation of Yoder and Sahama and signifies the molecular fraction as a percentage. All measurements on the silicon and olivine reflections were made above the two-thirds height, in order to measure the $\text{CuK}_{\alpha 1}$ contribution of the reflection. Measurements were made to 0.005° (2θ) using a standard engineering scale.

The corrected 2θ positions for 20 samples, calculated mol percent forsterite (Fo), and the standard deviation for each sample mean are presented in table 2. The significance of the standard deviation is simply that two-thirds of the values used in calculation of the arithmetic mean fall within $\pm s$ of the mean.

Analysis of X-ray Data

The precision of the x-ray determination of olivine composition has been estimated from 48 oscillations on two mounts of olivine crystals picked from kimberlite tuff from Buell Park (Allen

FIGURE 13

Determination curve and formula after Yoder and Sahama, 1957.

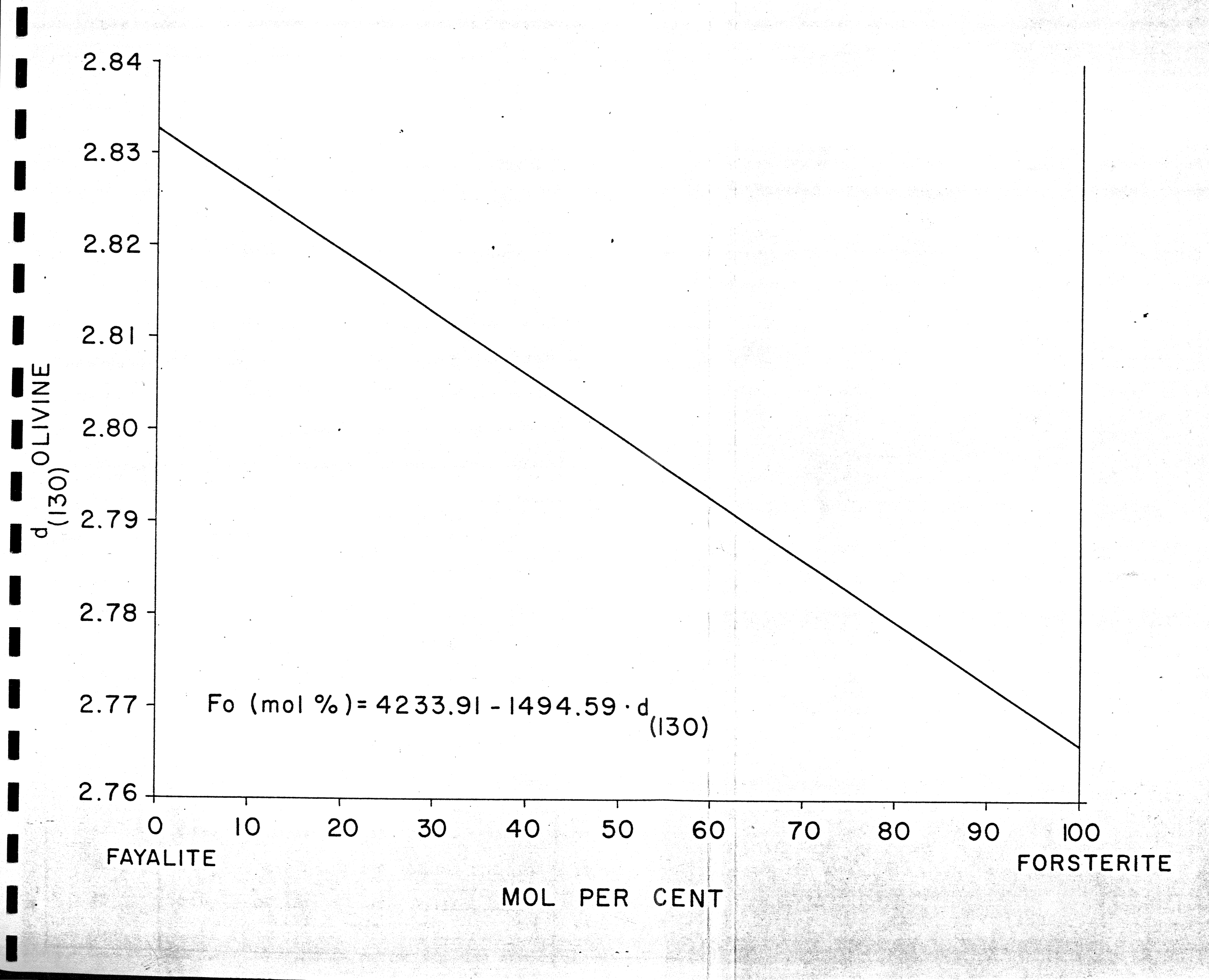


TABLE 2

Numbers 1 through 13 indicate sample localities, and letters following indicate sample position. Chip samples have no letter designation: T = top, M = middle, B = bottom, VB = very bottom, S = spheroidal zone and -X signifies the composition obtained from a single glomeroporphyritic clot. Numerical superscripts on sample means indicate the following:

1. The x-ray diffraction pattern showed split peaks, average was used.
2. Two mounts with four oscillations each, 79.8 ± 1.8 and 75.7 ± 0.8 .
3. Two mounts with four oscillations each, 77.3 ± 0.8 and 75.7 ± 0.9 .

TABLE 2. X-ray Determination on Parea Mesa Olivine Phenocrysts

Sample No. and Position	Flow Sampled	Corrected position of the olivine (130) using Si(111) of $28.440^{\circ}2\theta$ for $\text{CuK}\alpha_1$				Average Mol % Fo \pm S
1	QTb $\frac{1}{2}$ QTb ₁ ¹	32.170	32.155	32.160	32.175	78.0 \pm 1.0
1T	QTb	32.160	32.150	32.145	32.155	76.6 \pm 0.8
1T-X	QTb	32.135	32.140	32.175	32.175	77.1 \pm 2.8
1M	QTb ₁	32.150	32.160	32.135	32.140	75.8 \pm 1.4
1M-X	QTb ₁	32.175 32.200	32.175	32.170	32.179	80.4 \pm 1.6
1B	QTb ₁	32.155	32.155	32.155	32.135	76.6 \pm 1.6
2	QTb ₁	32.190	32.190	32.205	32.195	82.0 \pm 0.9
2T	QTb ₁	32.160	32.170	32.155	32.150	77.4 \pm 1.1
2T-X	QTb ₁	32.155	32.155	32.180	32.185	78.7 \pm 2.0
2M	QTb ₁	32.130	32.150	32.150	32.170	76.3 \pm 2.1
2B	QTb ₁	32.160	32.150	32.150	32.150	76.6 \pm 0.6
3	QTb ₂	32.150 32.140	32.160 32.135	32.145	32.140	75.7 \pm 1.1
3T	QTb ₂	32.155	32.160	32.170	32.170	78.1 \pm 1.0
3T-X	QTb ₂	32.170	32.150	32.150	32.150	77.0 \pm 1.3 ¹
3M	QTb ₂	32.160	32.175	32.175	32.175	79.0 \pm 1.0
3B	QTb ₂	32.165	32.170	32.170	32.175	78.9 \pm 0.5
4	QTb ₂	32.160 32.145	32.175 32.150	32.195 32.145	32.180 32.135	77.7 \pm 2.5 ²
4T	QTb ₂	32.140	32.155	32.160	32.165	77.0 \pm 1.3
4M	QTb ₂	32.130	32.150	32.160	32.165	76.5 \pm 1.9
4B	QTb ₂	32.180 32.150	32.180	32.155	32.155	78.1 \pm 1.8

TABLE 2. (Cont.)

Sample No. and Position	Flow Sampled	Corrected position of the olivine (130) using Si (111) of $28.440^{\circ} 2\theta$ for $\text{CuK}\alpha_1$				Average Mol % $\text{Fo} \pm \text{S}$
5	QTb ₂	32.170	32.145	32.205	32.190	79.8 \pm 3.2
5T		32.140	32.155	32.140	32.145	
		32.145	32.165	32.155	32.160	
		32.155	32.160			76.6 \pm 1.1
6	QTb ₂	32.150	32.160	32.140	32.130	75.7 \pm 1.6
6T	QTb ₂	32.160	32.160	32.170	32.155	
		32.160	32.155			77.6 \pm 0.7
6M	QTb ₂	32.105	32.125	32.120	32.120	
		32.110	32.120	32.115	32.115	72.0 \pm 0.8
6B	QTb ₂	32.130	32.140	32.140	32.165	
		32.165	32.175			76.6 \pm 2.4
6VB	QTb ₂	32.150	32.150	32.150	32.130	
		32.160	32.160	32.160	32.145	76.5 \pm 1.1
6S	QTb ₂	32.150	32.135	32.160	32.140	75.8 \pm 1.3
7	QTb ₂	32.160	32.160	32.130	32.155	76.5 \pm 1.9
7T	QTb ₂	32.170	32.165	32.145	32.140	76.9 \pm 1.9
7M	QTb ₂	32.140	32.155	32.155	32.160	76.7 \pm 1.1
7B	QTb ₂	32.140	32.145	32.150	32.160	
		32.170				76.7 \pm 1.5
8	QTb ₂	32.155	32.190	32.190	32.175	79.8 \pm 2.1
8T	QTb ₂	32.140	32.150	32.160	32.145	76.2 \pm 1.1
8M	QTb ₂	32.160	32.165	32.145	32.160	77.3 \pm 1.1
8B	QTb ₂	32.160	32.175	32.175	32.160	
		32.145	32.160	32.160	32.165	77.9 \pm 1.2
9	QTb ₂	32.195	32.190	32.170	32.185	80.8 \pm 1.3
9T	QTb ₂	32.170	32.170	32.185	32.190	80.0 \pm 1.3
9M	QTb ₂	32.140	32.150	32.150	32.160	76.3 \pm 1.0

and Balk, 1954). Approximately 5 grams of the light green variety of olivine were picked, crushed, ground and sieved. Of the sieved material, only the minus-44 micron fraction was used in the two mounts which were subsequently made. The mounting technique used was the same as described for the Parea Mesa basalt olivine, and silicon powder was used as an internal standard. The first mount was x-rayed, from 28° to 33° (2θ), 16 times during five separate runs. The second mount was x-rayed 32 times during seven separate runs. The results of these individual composition determinations are listed in table 3. The arithmetic mean of these two mounts is

$$\bar{x} = \frac{\sum x_i}{n} = 92.9 \text{ mol \% Fo,}$$

where the x_i 's are the composition determinations of each individual x-ray oscillation between 29° and 33° 2θ, and n is the number of oscillations. The standard deviation, s, is commonly referred to as the "students" standard deviation and is applicable in the analysis of small sample populations,

$$s = \frac{(\sum (x - x_i)^2)}{n - 1} = \underline{+2.2 \text{ mol \% Fo.}}$$

This value is close to the value given by Yoder and Sahama (1957), +2.45. The accuracy cannot be checked because only semi-quantitative chemical data is available for the major constituents of the Buell Park olivine, and no chemical data is available for the olivine of the Parea Mesa basalt. However, the x-ray determined composition

TABLE 3. X-ray Determination of Buell Park Olivine

Mount No.	Corrected Position of the olivine (130) using Si(111) of 28.440° 2θ for $\text{CuK}\alpha_1$				Average Mol %Fo \pm S
1	32.295	32.270	32.250	32.275	91.7 \pm 1.9
	32.285	32.265	32.270	32.290	
	32.275	32.275	32.270	32.270	
	32.275	32.250	32.295	32.245	
2	32.275	32.255	32.275	32.290	93.4 \pm 2.1
	32.310	32.255	32.280	32.290	
	32.290	32.305	32.285	32.290	
	32.290	32.305	32.285	32.295	
	32.290	32.295	32.290	32.300	
	32.280	32.315	32.295	32.300	
	32.270	32.260	32.285	32.305	
	32.245	32.265	32.285	32.310	
1 and 2	All the above				92.9 \pm 2.2

of the Buell Park olivine is in agreement with the optical determination of composition by Sun and Balk (in Allen and Balk, 1954), Fo 91 to 93 percent. Yoder and Sahara (1957) have estimated the accuracy of an individual observation to be ± 4 mol percent Fo near the pure end members, and ± 3 mol percent in the vicinity of 64 percent Fo.

Split peaks of the olivine (130) were noted in several instances (table 2) but no special significance was attached to these in the final analysis. Split peaks may indicate the presence of more than one compositional olivine phase, or a deviation in the instrumental reproducibility

of peak shapes. The investigation of this unusual feature was not pursued since it is beyond the scope of this paper.

In several instances olivine and bytownite clots of the grab samples were quite friable and easily picked from the surrounding groundmass. The samples from which clots were analyzed (table 2) for olivine composition were similar in composition to that obtained in the usual manner, with one exception, sample 1M-X. The determined composition for this sample was 5.6 mol percent richer in forsterite than sample 1M. This difference may or may not be significant; however, no explanation is offered.

The resultant compositions of the Parea Mesa basalt listed in table 2 were first scrutinized graphically, in order to examine the observed variations in olivine composition with regard to sample position and with respect to the olivine composition of composite chip samples. Figures 4 and 5 were constructed for this purpose and particular reference will be restricted to samples of flow QTb₂, unless otherwise specified. The results of analyses of olivine from sample localities 1 and 2 are included for completeness. After consideration of figure 4, several points of interest can be noted. For example: (1) 6 out of 11 of the top sample means are richer in Fo than those from the bottom, 8 of 11 of the top sample means are richer in Fo than those from the middle, and 6 of 11 of the bottom sample means are richer in Fo than the middle; (2) 19 out of 33 grab sample

Fe's are richer in Fe than the composite chip sample means for corresponding sample locations; and (3) only 17 out of 33, or 52 percent of the Fe values for grab sample means lie within the standard deviation of their corresponding composite chip sample means. Figure 5 also yields information concerning the relative variations of sample means, and, in addition, the arithmetic means of chip and position means are given for QTb₂. The plus, minus or zero nature of the slope between bottom, middle, top and chip samples for sample localities 3 through 13, or flow QTb₂, are shown in table 4. The arithmetic means of the four samples are different, with the mean of the top being greater than the bottom and the bottom greater than the middle. The arithmetic mean of the bottom, middle and top position means is 77.5 mol percent Fe, which is identical to the arithmetic mean of all chip samples of QTb₂.

TABLE 4. Slope Analysis of Figure 5

	3	4	5	6	7	8	9	10	11	12	13
Bottom	-	+	-	+	+	+	-	-	+	-	
Middle	-	+	-	+	+	-	+	0	-	-	
Top	-	-	+	0	-	+	+	-	-	-	
Chip	+	+	-	+	+	+	-	+	0	+	

FIGURE 10

Plot of apparent mol percent forsterite in Parea Mesa basalt samples. The composition obtained from the composite chip sample locality is represented by a vertical line with the lined area corresponding to the standard deviation. Circles and squares denote the relative stratigraphic position and apparent mol percent Fo for the grab samples.

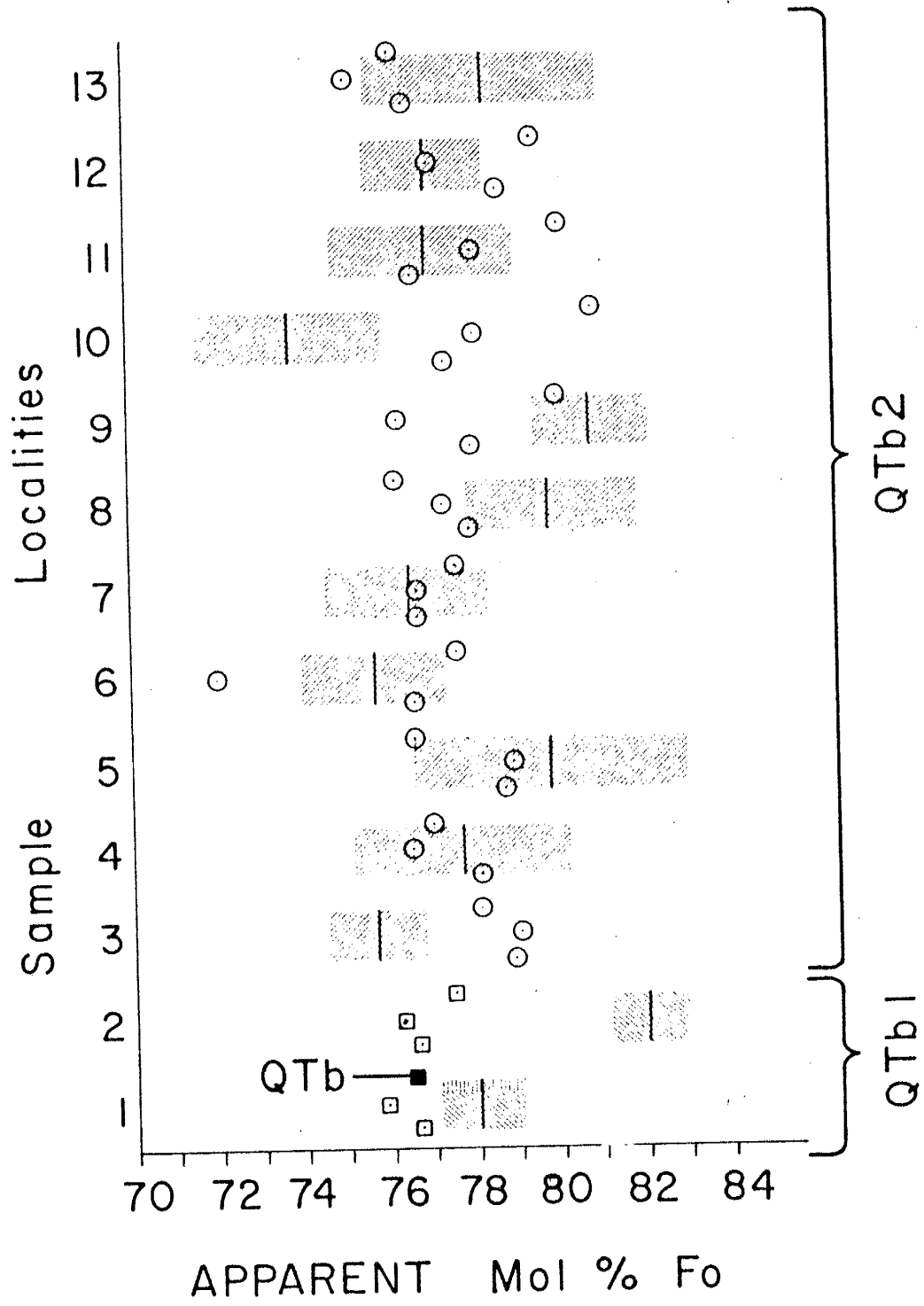


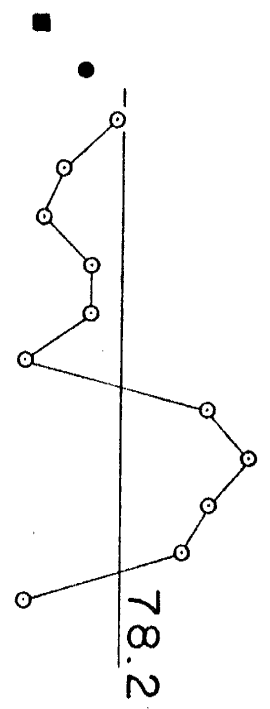
FIGURE 10

Variation in apparent mol percent Fo with respect to samples from the bottom, top, middle, and composite chip. The chip and position arithmetic means, are shown for QTb_2 and the sample means of QTb_1 (solid circles) and QTb (solid square) are also shown.

APPARENT Mol % F₀

72 74 76 78 80 82

Top

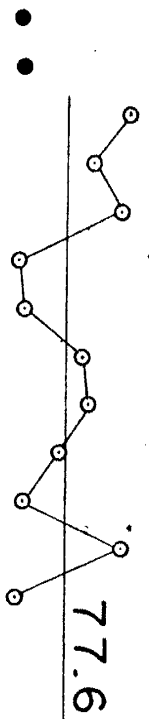


SAMPLE LOCALITIES

APPARENT Mol % F₀

72 74 76 78 80 82

Bottom

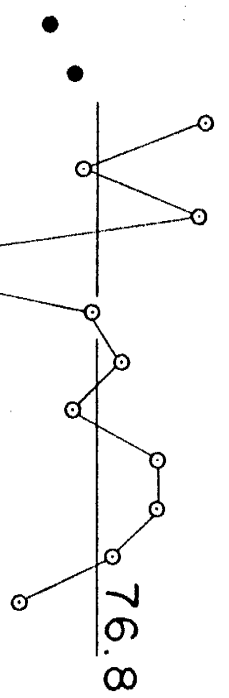


SAMPLE LOCALITIES

APPARENT Mol % F₀

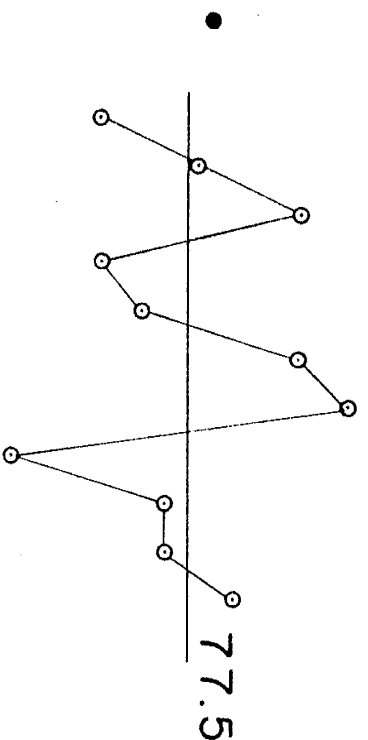
72 74 76 78 80 82

Middle



SAMPLE LOCALITIES

Chip



SAMPLE LOCALITIES

From the random variations shown in table 5 and the relatively discordant trends shown in figures 4 and 5, it appears that there is no systematic variation in olivine phenocryst composition with respect to position in the flow on an individual sample locality basis. However, there may be an over-all difference in the arithmetic means of position samples. This possibility was investigated in figure 6, which shows the distribution of sample means plotted with regard to sample position. These distributions appear to be normal about the arithmetic means shown and the range is less than $\pm 3s$. This deviation, $\pm 3s$, should include 99 percent of all samples in a normal distribution (Hoel, 1947). The arithmetic mean composition for each sample position is shown in figures 4 and 6; figure 6 also shows the standard deviation of each position mean. The standard deviations for each position mean are: ± 0.9 for bottom, ± 2.0 for middle, ± 1.7 for the top and ± 2.1 for the chips. The standard deviation for the 48 runs of Buell Park olivine was ± 2.2 so that the standard deviations for the position means are less than or equal to the standard deviation expected from a single olivine composition. The obvious conclusion is that there is no lateral variation in the composition of phenocryst olivine.

What of the vertical variation? Do the average compositions obtained show sufficient significant differences to conclude that there is vertical variation in composition? One may obtain some idea of

the significance of these position means if the 34 grab samples are combined into one arithmetic mean and its standard deviation, i. e. 77.5 ± 1.8 mol percent Fe . The arithmetic mean is the same as that obtained for the chip sample mean and the standard deviation is again less than the expected value of precision for an individual observation. The conclusion is that the position means represent normal variation in a single olivine composition population and that there is no significant difference in composition, vertically or horizontally, in the QTb_2 flow of Farea Mesa basalt.

These conclusions are amenable to certain statistical tests which will help determine their validity. For the statistical analysis only the first four oscillations from the x-ray analysis of each sample are used. This is necessary because all sample means were not determined using the same number of x-ray determinations of olivine composition and therefore some mean compositions may have been unduly weighted. The compositions obtained for each of the four oscillations for each sample are listed in table 6. The figures listed give equal weight to each sample and allow statistical evaluation of the position means and standard deviations. It is thought that the standard deviation calculated in this manner is more realistic and should be a better index to variation in the arithmetic means of each sample position. That is, if there is a variation in olivine composition in a lateral sense, the standard deviations realized from the

FIGURE 6

Histograms of the apparent mol percent Fe with regard to bottom, middle, top, and chip and all of these for flow QTb₂ plus the histogram of all samples from QTb. The arithmetic mean is denoted by a vertical arrow and the standard deviation by the length of a horizontal bar.

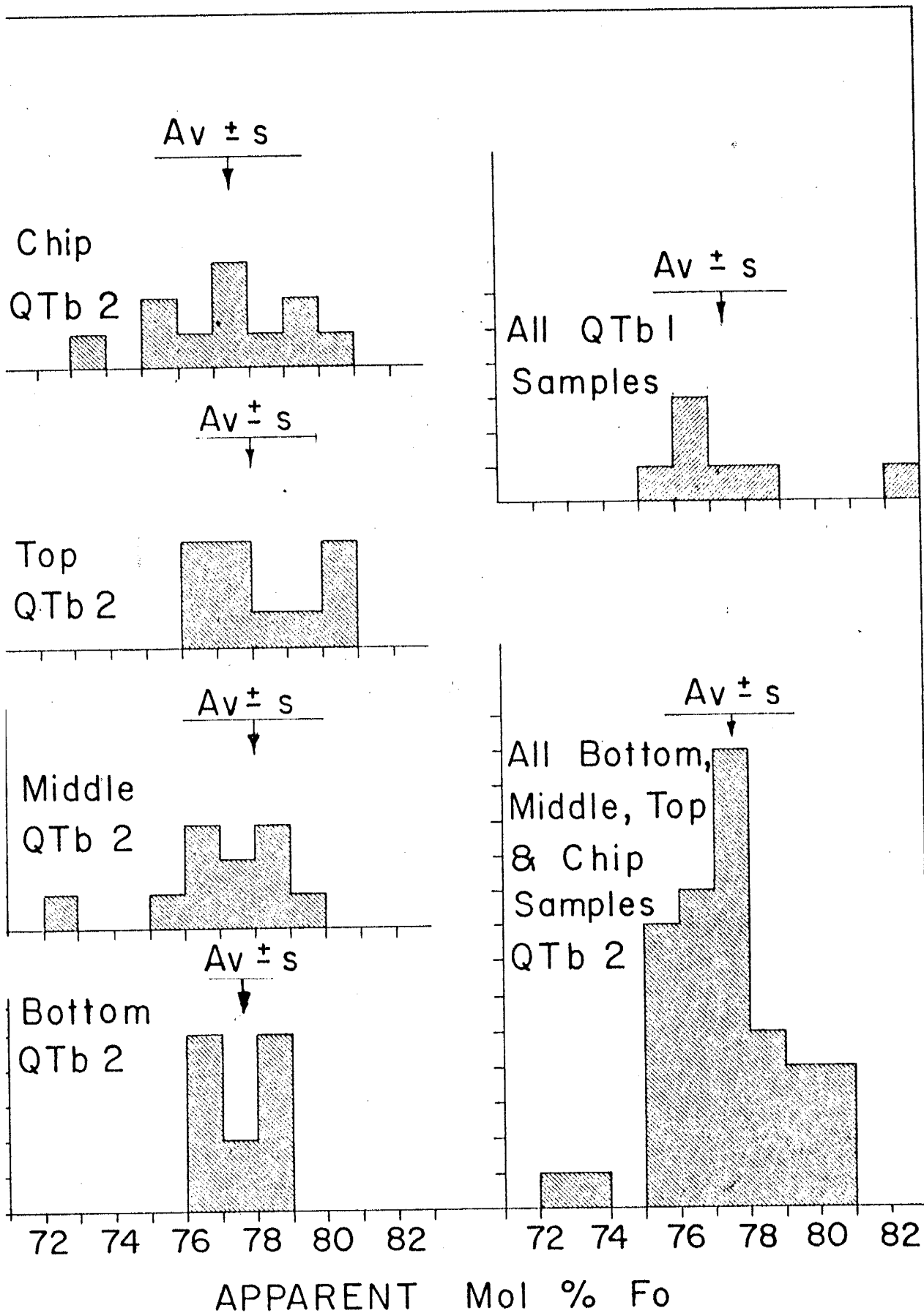


TABLE 5. X-ray Compositions Obtained in the First Four Oscillations
for Statistical Analysis of Data
(in mol % Fo)

SAMPLE LOCATIONS

Sample Location	Grab Samples			Chip	Spheroidal Zone	Other, Description	
	Bottom	Middle	Top				
Samples from QTb ₁	77.0	76.3				79.5	Glomero- phenocryst from IM
	77.0	77.6				79.5	
	77.0	74.4				78.9	
	74.4	75.1				81.4	
	77.6	73.8	77.6	81.4		77.0	Glomero- phenocryst from 2T
	76.3	76.3	78.9	81.4		77.0	
	76.3	76.3	77.0	83.3		80.1	
	76.3	78.9	76.3	82.0		80.8	
±S	76.5±1.0	76.1±1.7	77.4±1.1	82.0±0.9		79.3±1.6	
±S for all grab samples from QTb ₁ = 76.5 ± 1.4							
Samples from QTb ₂	78.2	77.6	77.0	77.6		78.9	Glomero- phenocryst from 3T
	78.9	79.5	77.6	76.3		76.3	
	78.9	79.5	78.9	75.7		76.3	
	79.5	75.5	78.9	75.7		76.3	
	80.1	73.8	73.8	76.3 ¹			
	80.1	76.3	76.3	75.7			
	77.0	77.3	77.6	75.7			
	77.0	78.2	78.2	74.4			
	78.9	77.6	75.1 ¹	78.9			
	78.9	77.6	77.0	75.7			
	78.9	80.8	75.1	83.3			
	78.2	79.5	75.7	81.4			
	73.5	70.7	77.6	75.1	76.3	76.3	Additional sample from very bottom. (Included in bottom posi- tion mean)
	75.1	73.1	77.6	73.8	74.4	77.6	
	75.1	72.5	78.9	76.8	77.6	74.4	
	78.2	72.5	77.0	77.8	75.1	75.7	

SAMPLE LOCATIONS

Locality	Grab Samples			Chip	Spheroidal Zone	Other, Description
	Bottom	Middle	Top			
	78.9 77.6 76.3 75.1	75.1 77.0 77.0 77.6	75.1 78.9 78.9 78.9	77.6 77.6 73.8 77.0		
	77.6 79.5 79.5 77.6	77.6 78.2 75.7 77.6	75.1 76.3 77.6 75.7	77.0 81.4 81.4 79.5		
	77.0 77.0 78.2 78.2	75.1 76.3 76.3 77.6	78.9 78.9 80.8 81.4	82.0 81.4 78.9 80.8		
	76.3 77.0 77.6 78.9	75.1 77.0 79.5 80.8	79.5 80.8 81.4 81.4	75.7 76.3 70.7 71.9	76.3 77.6 77.6 73.8	
	79.5 77.3 77.3 75.1	76.3 78.2 78.9 78.9	78.9 80.1 81.4 81.4	75.1 76.3 80.1 76.3	73.8 75.1 76.3 77.6	
	77.0 78.2 78.9 80.8	74.4 75.1 78.9 80.1	78.9 78.2 80.8 80.2	75.1 77.0 77.6 78.5		
	75.7 ¹ 74.4 76.3 76.3	73.8 75.1 75.7 76.3	75.7 76.3 75.7 77.0	73.8 80.8 79.5 79.5	71.9 75.1 77.6 73.1	

\pm S 77.5 \pm 1.7 76.8 \pm 2.3 78.1 \pm 2.0 77.6 \pm 2.8 75.6 \pm 1.8 Not calculated
(Position means for first four oscillations of each sample)

\pm S 77.6 \pm 0.9 76.8 \pm 2.0 78.2 \pm 1.7 77.5 \pm 2.1 75.5 \pm 1.0
(Position means from the sample means of Table 2)

\pm S for all grab samples using first four oscillations 77.5 \pm 2.0
 \pm S for all grab samples using sample means 77.5 \pm 1.8

TABLE 5. (Continued)

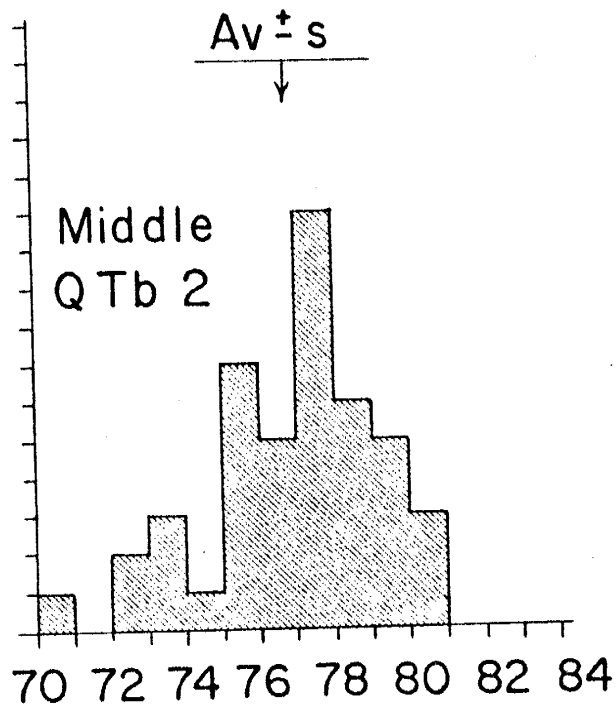
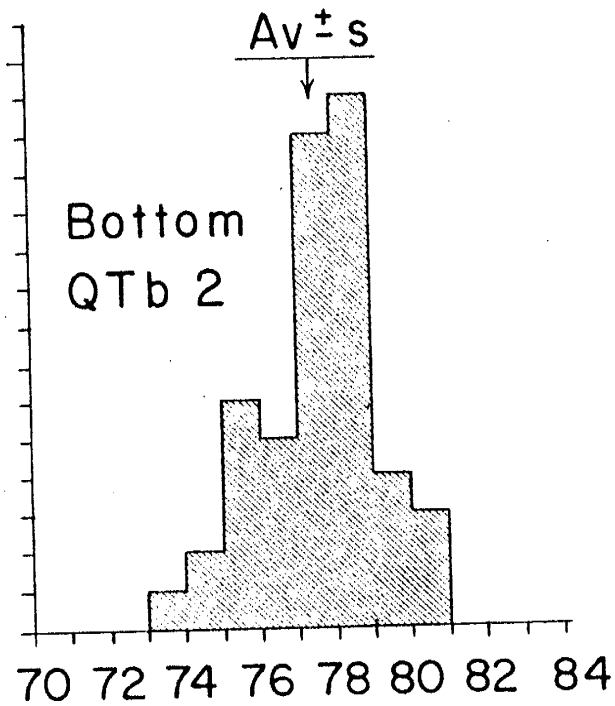
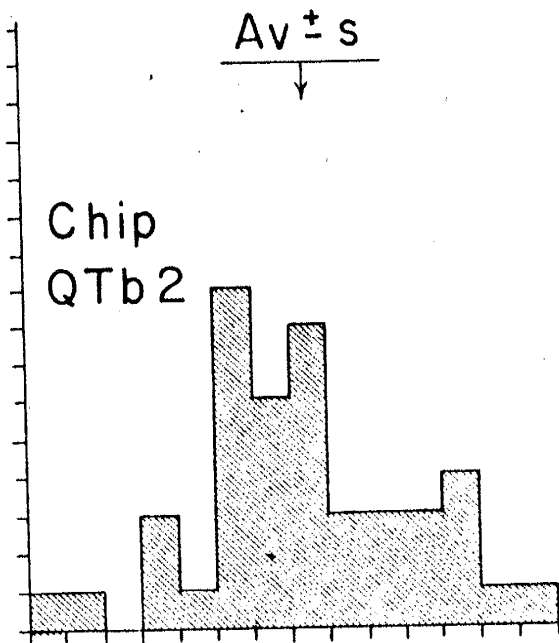
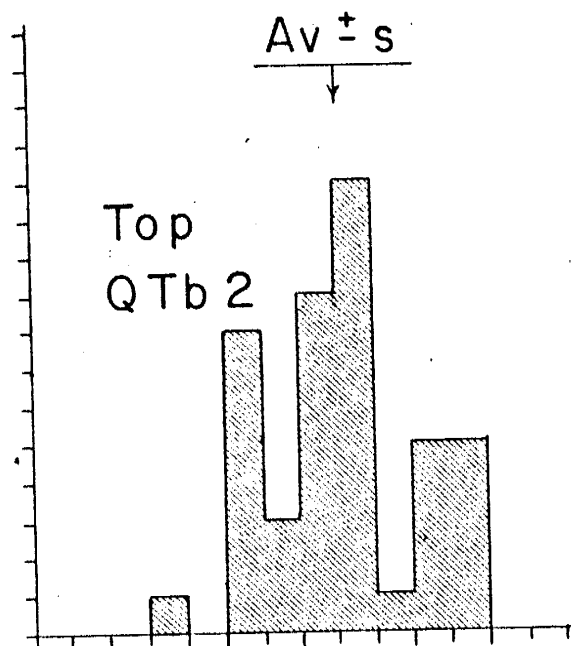
Other Areas Sampled

Sample quality	Sample number	QTb	Sample number	Zuni Salt Lake	Little Black Peak	Carrizozo	Cerro Verde
Calculated composition for each oscillation	IT	77.6	SL-1	83.9	78.2	79.5	76.3
		76.3		85.1	78.9	78.2	76.3
		75.7		82.0	77.6	75.7	73.1
		77.0		82.0	78.2	77.0	75.1
	ITX	74.4	SL-2	82.7			
		75.1		81.4			
		79.5		82.0			
		79.5		80.1			
			SL-3	79.5			
				78.9			
				86.3			
				87.3			
M. †S	77.1 [†] ±2.8		82.6 [†] ±2.6	78.4 [†] ±0.2	77.6 [†] ±1.7	75.2 [†] ±1.5	

† Denotes that first four oscillations were obtained from the second mount of this material.

FIGURE 7-11

The frequency distributions of the first four oscillations for the position means of QTb_2 and the chip mean. The vertical arrow indicates the arithmetic means of these distributions and the horizontal line indicates the standard deviation.



APPARENT Mol % Fo

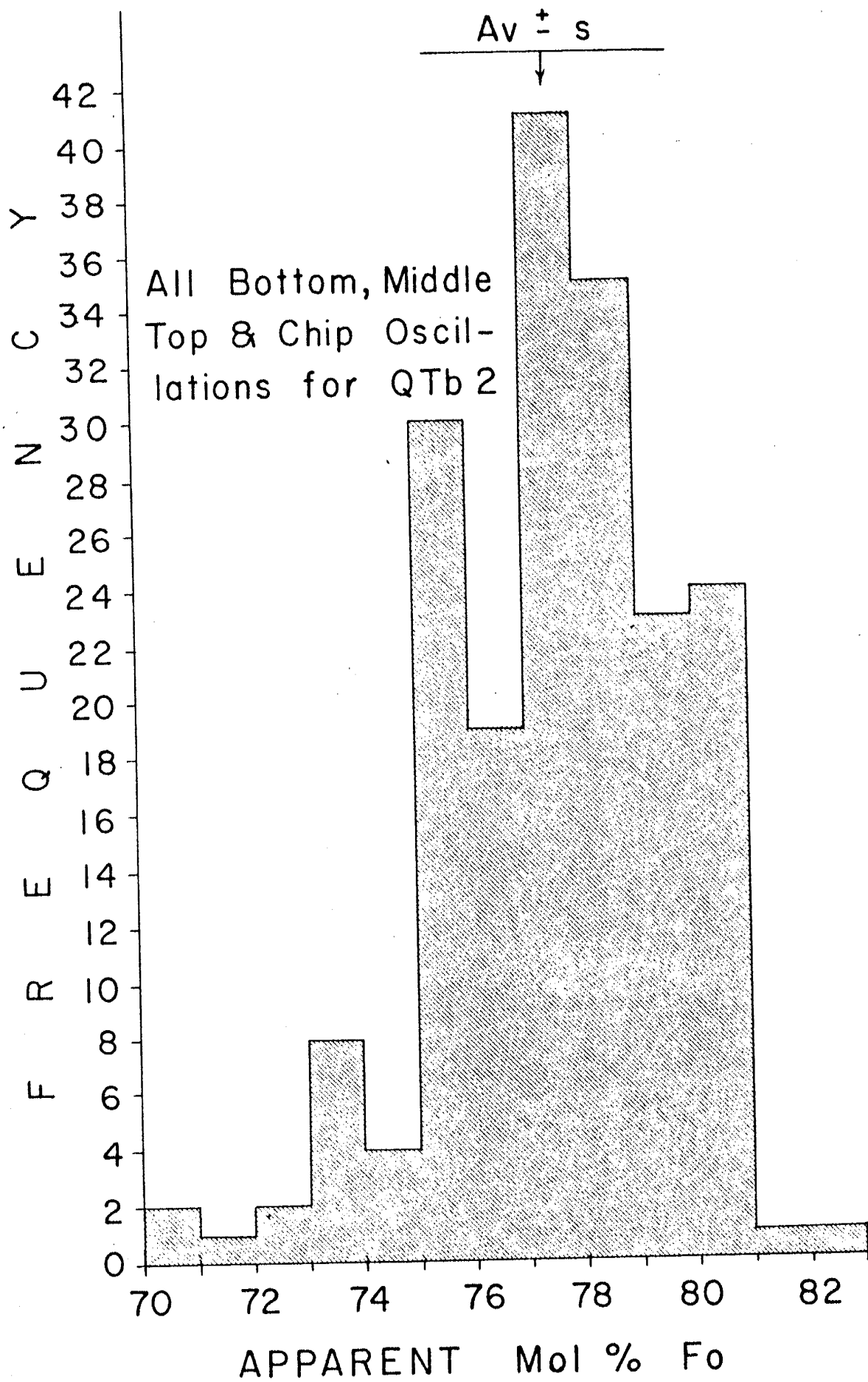
first four oscillations (per sample) should be greater than that expected for one composition population, probably +3.0 or greater. At the same time the position means obtained from the first four oscillations (per sample) should not deviate greatly from the position means obtained from sample means of table 2, shown in figures 5 and 6, which are based on four to ten oscillations per sample. In addition, the distribution of compositions about each of the position means should be normal, i.e. similar to the distribution shown in figure 6. The comparison of position means is shown in table 5. The distributions of compositions which comprise the population of values from which these means were obtained are shown in figures 6 and 7.

The position means, shown in table 5, for the QTb_2 flow of Parea Mesa basalt are very similar to the position means obtained from the sample means of table 2. These means correspond to within + 0.1 mol percent Fo . From this it is concluded that more than four oscillations are probably not warranted in the determination of sample means. However, for the determination of any one sample mean ten oscillations are better than four. The deviation using a lesser number of oscillations or determinations has not been investigated.

The standard deviation obtained from the first four oscillations without using the calculated sample mean of each sample is greater than when the standard deviation was calculated using sample

FIGURE 8

The frequency distribution of the olivine compositions as determined from the first four oscillations for all bottom, middle, top and chip samples of QTb₂. Vertical arrow indicates the arithmetic mean and the horizontal bar indicates the standard deviation.



means, table 2. But, in spite of this increase in standard deviation the resultant value is similar to or less than the expected deviation for single observation (+2.2 mol percent Fo). Only the standard deviations of the chip and middle means are greater than the expected value, and even then the difference is slight. It can be concluded therefore that the lateral variations in the Parea Mesa basalt flow QTb₂ are within the expected value of precision for one composition population for the chip, bottom, middle, and top sample positions. This conclusion is further supported by the normal distributions of compositions shown in figure 8.

The fact that the position means are different still leaves the possibility of vertical variation to be considered. The first test of this variation is obtained by calculating a grab sample mean of the first four oscillations for all bottom, middle and top grab samples (table 5). The mean obtained is the same as that calculated using sample means of table 2, and is very close to the chip mean obtained from both methods. Probably of more significance is the fact that the standard deviation of the grab sample mean obtained from the first four oscillations of all bottom, middle and top grab samples of QTb₂ is less than the expected value of one composition population. By the same token the distribution of all grab and chip samples is normal, as shown in figure 8, and the standard deviation is the same as the expected value for one composition population. Again this strongly suggests that there is but one composition population of olivine in the Parea Mesa flow of QTb₂.

The theorems of statistics can determine whether the position means of QTb_2 belong to the same statistical population or whether they represent different sample populations. The methods used herein are commonly referred to as the F-test and the t-test (Hoel, 1947). The F-test is used to test the variances (i.e. variance equals s^2) of two sample populations. The t-test is utilized to test the equivalence of the mean values of two sample populations. A necessary and sufficient condition for the application of the t-test is a nonsignificant F-test. For sample populations the value of F can be calculated by the following formula (Hoel, 1947):

$$F = \frac{n_x s_x^2 / n_x - 1}{n_y s_y^2 / n_y - 1}$$

where n_x and n_y are the number of individuals in each group and s_x^2 and s_y^2 are the respective variances. A null hypothesis is postulated when the F-test is used, and proof of the hypothesis is realized by a nonsignificant F-test. When the calculated F is less than the tabulated value, for the same degree of freedom (found in tables of any standard statistics text; Hoel, 1947), the F-test is nonsignificant. The degree of freedom is found from the number of individuals in each group; each mean then has a degree of freedom equal to its numerical size.

In relatively small numbers of samples, the Student's t-test (Hoel, 1947) is used to test the equality of sample means,

$$t = \frac{\bar{x} - \bar{y}}{(n_x s_x^2 + n_y s_y^2)^{1/2}} \left[\frac{n_x n_y (n_x + n_y - 2)}{n_x + n_y} \right]^{1/2}$$

A null hypothesis is also postulated in application of the t-test and proof of the hypothesis is a nonsignificant t-test at the closed confidence level and same degree of freedom as that listed in a standard statistics text, (Hoel, 1947). Here again a nonsignificant test is indicated by a calculated value which is less than the listed table value. A nonsignificant t-test suggests that the compared sample means belong to the same sample population while a significant t-test indicates that the sample means are of different populations.

In order that the F-test and the t-test be valid it must be assumed, or otherwise inferred, that the distribution of position sample means is normal and that the sample population, from which the position means were obtained, is representative. Position means refer to the arithmetic means of the bottom, middle, top and chip sample means, and sample means refers to the population from which the position means were obtained. That is, each sample has an arithmetic mean, as listed in table 2, based on four to ten oscillations. The distribution of sample means is represented by the histograms of figure 6. The distributions shown have normal to bimodal tendencies, while the distributions of figure 8 appear to be all unimodal and normal. The bimodal tendency of figure 6 may be reflected by the small number

of sample means used in the histograms of the position frequencies, while those of figure 8 are based on four times as many composition determinations. The fact that all distributions have ranges less than $\pm 3s$, where s is the expected value of one normal population, suggest that the distributions of figures 6-8 are normal. Figure 9 shows the distribution of the individual composition determinations used in calculating the mean for two mounts of the Buell Park olivine. Both distributions appear to be normal and the combination of both mounts yields (figure 10) a standard deviation which is less than that given by Yoder and Sahama (1951) for the precision of one individual determination, so there is good reason to infer the equivalence of the means obtained from these two mounts. It is believed that if any differences did exist between these two mounts, the standard deviation of the entire population would be greater than the value of Yoder and Sahama (1957, 2.45 mol percent Fo).

The problem of obtaining a representative sample is, and probably always will be, subject to question until more samples are available, but for statistical considerations 11 samples will be assumed to be sufficient for the testing of position populations. Table 6 lists the results of the statistical analysis carried out at the 90 percent confidence level.

In any statistical analysis of this type the choice of confidence level is always a problem. This problem arises because a very high

confidence level only distinguishes between extreme differences, while at low confidence levels insignificant differences will be indicated as significant. For example, at the confidence level of 99 percent the test will only be in error 1 percent of the time. And at a confidence level of 50 percent the result will be in error 50 percent of the time. In the statistical analysis of olivine phenocryst composition, it is hoped that a confidence level of 90 percent will be applicable for the distinction of similar and dissimilar data.

The means used in table 6 were obtained from tables 3 and 5 for the Buell Park olivine and those of the Parca Mesa, respectively. The statistical analysis of Buell Park olivine reveals that both mounts have means which are members of the same composition population. Therefore the author feels justified in using the standard deviation of ± 2.2 , after consideration of all oscillations of both mounts as one composition population.

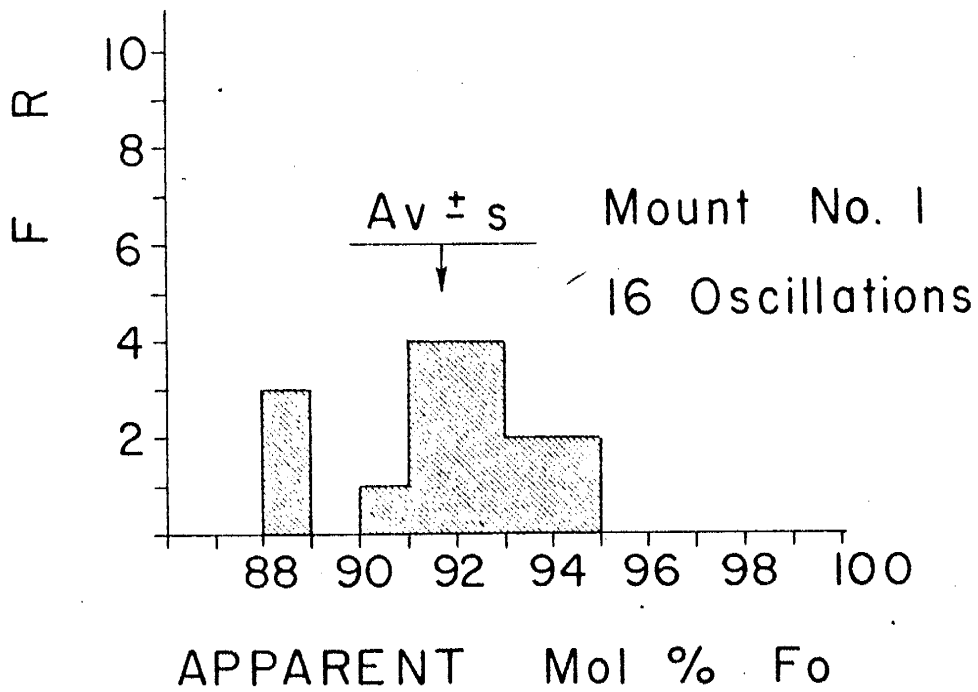
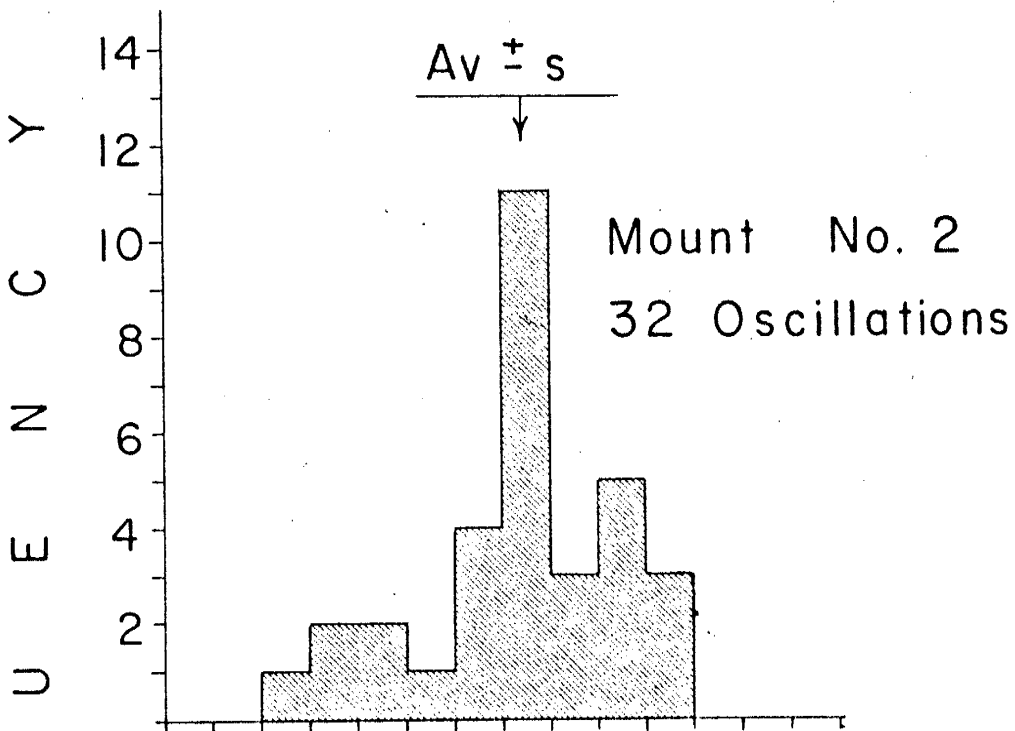
In the analysis of QTb_2 of the Parca Mesa basalt the chip mean was found to belong to the same composition population as all the grab sample means. In addition, the position means of all grab samples were compared with each other and no population difference was apparent between them.

However, when the sample mean of samples from spheroidal zones are compared with the other means of QTb_2 samples, at least some dissimilarities are found. The position mean of the top of QTb_2 and the grab sample mean of QTb_2 show significant differences

FIGURE 9

FIGURE 9

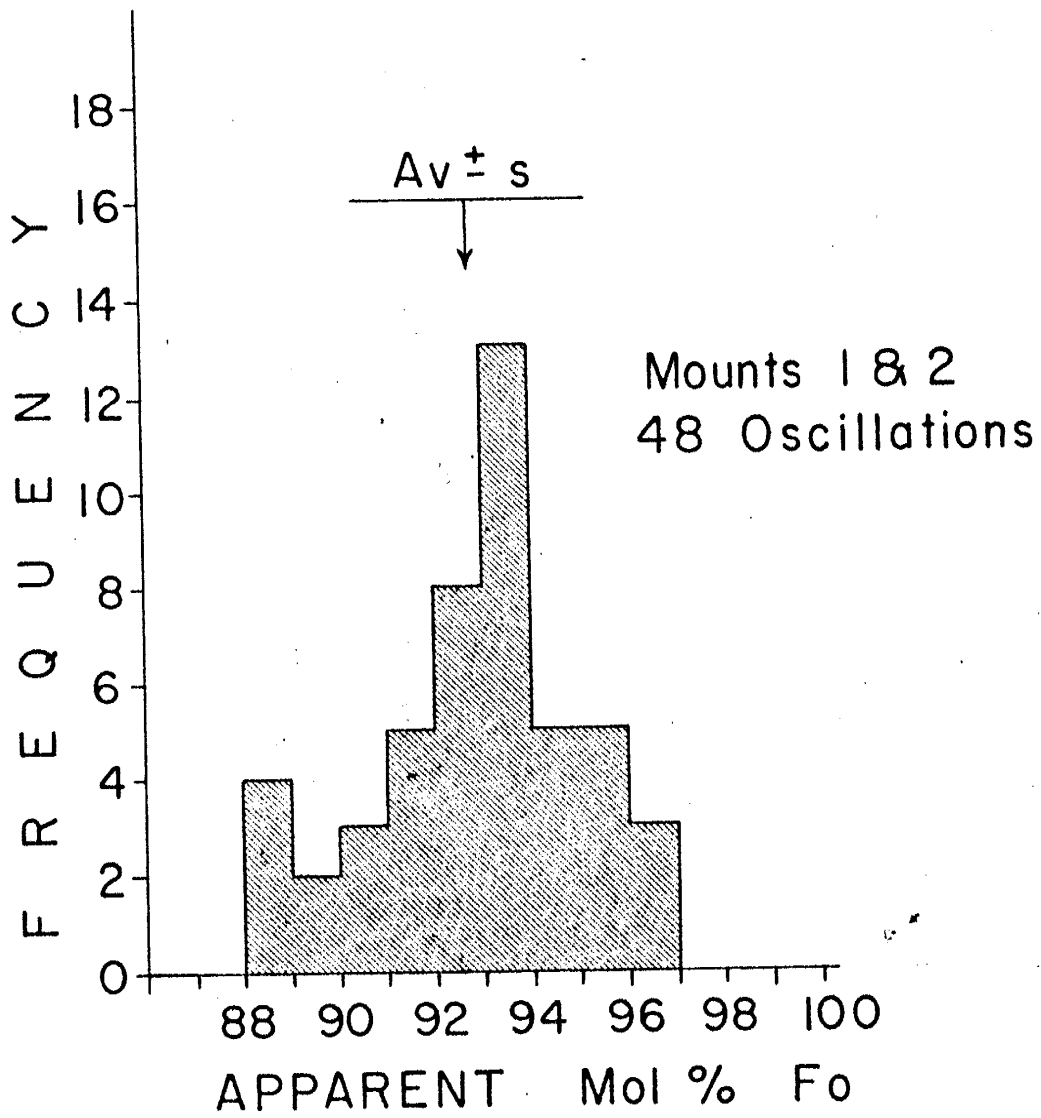
Illustrates the histograms of two mounts of olivine picked from a kimberlite tuff from Buell Park (Allen and Balk, 1954). Vertical arrow indicates the arithmetic mean and the horizontal bar indicates the standard deviation.



OF IRON

FIGURE 10

The frequency distribution of all first and second mount oscillations which were used in calculating the composition of Buell Park olivine. Arrow indicates the arithmetic mean of these oscillations and the horizontal bar indicates the standard deviation of the distribution.



with the sample mean of spheroidal zone samples. In addition, the difference between the other sample means becomes significant at slightly lower confidence levels of 89 percent for the chip mean, 82 percent for the bottom mean, and 59 percent for the middle mean. The spheroidal zone mean thus appears to be different from the grab sample mean, the chip mean and the top and bottom position means; while it is similar to the middle position mean. This confirms the correlation between these two sample areas as far as hand specimen appearance is concerned. Likewise, in thin-section the alteration between these two areas is similar.

Two objections to the correlation of these two sampling positions may be raised: first, the middle position means may be lowered by the inclusion of samples from central spheroidal zones which were not expressed on the outcrop surface; and secondly, the spheroidal zones may not be adequately sampled to define the mean. If it is assumed that these objections are unwarranted then one might be able to correlate mean olivine phenocryst compositions with the intensity of alteration. That is, the most intense to least intense alteration would be; spheroidal zones, middle positions, bottom positions and top positions. The composition of the olivine phenocryst fraction seems to decrease in Fo content with increase in alteration. This might be explained by more rapid alteration of forsterite rich phenocrysts or zones in phenocrysts. In addition

TABLE 6. Statistical Comparison of Data at the 90 Percent Confidence Level
(Considering the Right-Tail Only)

Location of Samples	Number of Samples	Number of Oscillations	Mol % Fo AM \pm S ¹	F-test	t-test
Park (1)	1	16	91.7 \pm 1.9	Nonsignificant	Nonsignificant
2 (2)		32	93.4 \pm 2.1		
Mesa					
Location					
ns of					
2					
tip	11	44	77.6 \pm 2.8	"	"
bottom	12	48	77.5 \pm 1.7		
tip	11	44	77.6 \pm 2.8	"	"
middle	11	44	76.8 \pm 2.3		
tip	11	44	77.6 \pm 2.8	"	"
top	11	44	78.1 \pm 2.0		
bottom	12	48	77.5 \pm 1.7	"	"
middle	11	44	76.8 \pm 2.3		
bottom	12	48	77.5 \pm 1.7	"	"
top	11	44	78.1 \pm 2.0		
middle	11	44	76.8 \pm 2.3	"	"
top	11	44	78.1 \pm 2.0		
. Z. ²	4	16	75.6 \pm 1.8	"	"
tip	11	44	77.6 \pm 2.8		
. Z.	4	16	75.6 \pm 1.8	"	"
bottom	12	48	77.5 \pm 1.7		
. Z.	4	16	75.6 \pm 1.8	"	"
middle	11	44	76.8 \pm 2.3		
. Z.	4	16	75.6 \pm 1.8	"	Significant
top	11	44	78.1 \pm 2.0		

(Continued)

TABLE 6. (Continued)

Location of Samples	Number of Samples	Number of Oscillations	Mol % Fe AM [±] S ¹	F-test	t-test
S. M. ³ Z	34 4	136 16	77.5 [±] 2.0 75.6 [±] 1.8	Nonsignificant	Significant
Comparison of with other mesa flows					
G. S. M. G. S. M.	34 5	136 20	77.5 [±] 2.0 76.5 [±] 1.4	"	Nonsignificant
G. S. M. G. S. M.	34 1	136 4	77.5 [±] 2.0 76.6 [±] 0.8	"	"
Comparison of with sam- ple other s					
S. S. M. Butte	34 1	136 4	77.5 [±] 2.0 78.4 [±] 0.2	Significant	<u> </u>
S. S. M. Zozo	34 1	136 4	77.5 [±] 2.0 77.6 [±] 1.7	Nonsignificant	Nonsignificant
S. S. M. Verde	34 1	136 4	77.5 [±] 2.0 75.2 [±] 1.5	"	"
S. S. M. Salt Lake	34 3	136 12	77.5 [±] 2.0 82.6 [±] 2.6	"	Significant

[±]S is the arithmetic mean and standard deviation.

Z. signified those samples from known spheroidal zones.

M. is the grab sample mean.

the intensity of alteration may be an index to the degree of retention of deuteric solutions, that is, retention of deuteric solutions appears to have been at a maximum for spheroidal zones. However, it cannot be concluded that this is the entire explanation for the phenomenon. The inclusion of, and reaction with, autoliths material may also be effective since this material may contain olivines of slightly different forsterite content, both mechanisms are probable.

Variation of olivine phenocryst composition between flows was not thoroughly investigated in this study; however, some samples were obtained from flow QTb₁ and the bottom flow of QTb of the Parea Mesa sequence. The comparison of these samples with QTb₂ is shown in table 6. There does not appear to be any significant difference between the means of these samples. Thus, there is no obvious variation in the composition of olivine phenocrysts in all the flows of the Parea Mesa basalt which have been sampled; however, more data is required to substantiate this conclusion.

Differences in composition of olivine phenocrysts in olivine basalt from other areas have been recognized and are tabulated in table 6.

The sample from Black Butte was obtained from the approximate crest of the butte one mile south of U. S. Highway 60, about eight miles east of Bernardo, New Mexico. The sample from the Cerro Verde flow is from the northeastern portion of the Mesa

del Oro quadrangle of Socorro and Valencia counties, which has been mapped and described by Jicha (1948); the sample position in the flow is unknown. The sample from the Carrizozo flow was obtained from the north side of a road cut along U. S. highway 380 within the flow. The three samples from the Zuni Salt Lake area (Darton, 1905) were collected from: the interior of the western cone, on the eastern side and roughly ten feet above the water line; the approximate crest of the eastern cone; and from the approximate center of a possible cone between these two cones, which has been leveled for the purpose of making a dam. Zuni Salt Lake is in the north-central portion of the Canon Largo quadrangle, which has been mapped by Willard and Weber (1958).

These scattered localities were not sampled in detail, but the comparison of composition means suggest that olivines from the Carrizozo flow and the Cerro Verde flow belong to the same composition population as flow QTb₂ of Parea Mesa. The phenocryst olivine composition of the Zuni Salt Lake area appears to be of a different population, and the composition of olivine phenocrysts of the Black Butte area cannot be compared because of a significant F-test. This comparison is speculative, due to the nature of the sampling and other properties may be used to differentiate these flows, but there does appear to be some variation in the olivine

phenocryst composition from flow to flow. Therefore the use of phenocryst composition may be a valuable aid in subsequent petrographic studies of olivine-bearing basalts. It is not proposed that the olivine phenocryst composition of olivine-bearing basalts be used as the sole property for distinguishing or correlating, but as a supplement to other petrographic data.

In general, lava flows may still exhibit compositional variations in olivine in a vertical and lateral sense, regardless of the results of this study, but careful sampling should readily delineate the changes. The most representative sample of a flow, where vertical exposures are present, is the chip sample method. However, in some localities bottom, middle and top samples should be taken in order to obtain an idea of the possible vertical variations. If the standard deviation calculated from such grab samples is less than the expected value of precision of an individual observation then the vertical variation is probably insignificant. Subsequent grab samples obtained from the same flow should be collected with regard to sample position in the flow, and may be used for investigation of lateral variations in the flow. Four samples need not be taken at every sampling locality. For example, if the investigation is restricted mainly to top samples the average and standard deviation of these could furnish an index to the lateral variation in this plane

of the flow. If a series of vertical grab samples could be obtained for several sample localities one would have an idea of the vertical variation from top to bottom. Statistical comparisons could then be drawn between sample positions for an indication of the lateral variation in other planes of the flow. Other features of a flow, such as alteration zones and xenoliths, might also be examined using similar techniques.

SUMMARY

The author mapped a portion of Parea Mesa and examined several of the basalt flows found thereon. Relationships between the underlying beds of volcanic sediments and the Parea Mesa basalt flows QTb₁ and QTb₂ were investigated.

Approximately 15,000 feet of exposures of Parea Mesa flows QTb₁, QTb₂, and QTb were sampled. Flow QTb₂ was sampled most intensively in order to study the possible vertical and lateral variations in physical properties and phenocryst olivine composition in a single flow.

The composition of olivine phenocrysts was determined utilizing the method and determinative curve of Yoder and Sahama (1957) for natural olivines. Complete chemical analyses of the olivine samples were not available but the apparent compositions of olivine phenocrysts shows insignificant variation between different localities and positions in the Parea Mesa basalt flows; spheroidal zones are possible exceptions to this generalization. Statistical comparisons made between phenocryst olivine compositions from spheroidal zones in QTb₂, from the other flows of Parea Mesa and from olivine basalt flows from scattered localities in other parts of central and western New Mexico, indicate significant differences in some cases. The similarities and differences should be an aid in the study of olivine-bearing basalts.

CONCLUSIONS

Flows QTb₁ and QTb₂ are conformable to a possible basin (Parea Mesa basin) formed in the underlying beds of volcanic sediment in the southwestern portion of the field area. In the northern and eastern portions of the field area the structure of the underlying beds is essentially horizontal or dips gently eastward. The field relationships of the flow QTb₁ and QTb₂ indicate that QTb₁ is essentially confined to the southern part of the postulated Parea Mesa basin, while flow QTb₂ has apparently filled the northern part of the basin and extended out onto a horizontal surface to the north and east. Subsequent flows (QTb and QTb₃) have been extruded from the southern portion of the field area in the vicinity of Parea Mesa, but these flows do not show a co-extensive development with QTb₂. Wright (1946) proposed a late Pliocene age for Parea Mesa basalt and believes the area has been exhumed. Scattered pebbles and gravel layers overlying QTb₂ are believed to be relicts from a veneer over Wright's (1946) Segundo Alto surface.

The laboratory investigation of samples obtained from Parea Mesa basalt flow QTb₂ reveal several variations with regard to sampling position.

The gross hand specimen color varies from the bottom, middle and top of the flow. Bottom hand specimens are dark gray to black, middle hand specimens are dark-bluish to greenish-gray

and top hand specimens are light gray to light brownish gray. The gross color of hand specimens from these various positions is believed to be due to the extent and type of alteration.

Alteration in the very bottom portions of the flow yielded a groundmass of black, opaque crystallites inferred to be iron-rich. This alteration is believed to be principally due to a combination of deuteric solutions and contamination of solids, gases and possible fluids, from the underlying sediments.

Alteration in the middle portion of the flow yielded a dark green structureless product, an olive green fibrous to microcrystalline product, and a light green fibrous microcrystalline product. The dark green material was found in areas of most intense alteration where it commonly forms pseudomorphs after olivine. The olive green alteration product forms from olivine and groundmass plagioclase. The light green alteration product fills interstices between groundmass plagioclase. Mineralogically all these green alteration products appear similar to smectite-chlorite described by Wilshire (1958). The color change of alteration products from green to red is thought to indicate a change in mineralogy, smectite-chlorite to goethite, and thereby becoming iddingsite. This same phenomenon has been observed by Wilshire (1958).

Spheroidal zones represent locales of intense alteration of the green type. Where such zones are closely associated with frac-

tures, the fractures may show no relation to the color changes in the altered zones. The present study has not attempted a solution of the origin of the spheroidal zones.

The alteration in the upper portion of QTb_2 is much less intense and is essentially restricted to reddish iddingsite after olivine, and calcite after plagioclase feldspars.

The time and nature of alteration which has yielded this complex aggregation of alteration products is thought to be late-stage deuteric solutions with minor subsequent changes due to weathering. The detailed explanation of environment and mineralogy are beyond the scope of this study.

The shape, size and volume percentage of vesicles in QTb_2 varies with position in the flow, as does the mineralogy of the amygdules. The relative amount of vesiculation is greatest at the bottom, less at the top and least in the middle portions of the flow. The vesicles are flat to elliptical at the top and bottom of the flow, while those in the middle portion are usually spherical. Bottom vesicles are irregular in outline with very rough interiors which are bright red and partially filled with calcite. Top vesicles are bounded by a relatively smooth interior. The top amygdules contain clear to milky calcite. The amygdules of the middle portion of the flow are calcite with varying proportions of iron-bearing montmorillonite.

The modes from various positions with QTb₂ are believed to be essentially the same; only the intensity and type of alteration is variable.

No systematic differences were found between the sample means of olivine phenocryst compositions from various sample positions in flow QTb₂. Position means, calculated from the first four x-ray oscillations, define a mean which does not deviate greatly from the position mean calculated from sample means, where sample means are based on four to ten x-ray oscillations. The position means for the bottom, middle and top of flow QTb₂ are 77.5 ± 2.3 and 78.1 ± 2.0 mol percent Fo, respectively, and the composite chip sample mean is 77.6 ± 2.8 . The arithmetic mean of four samples obtained from spheroidal zones in QTb₂ is 75.6 ± 1.8 mol percent Fo. At a confidence level of 90 percent the chip sample mean and all position means appear to belong to the same composition population. The composition population which is believed to be most representative for the Parea Mesa QTb₂ basalt flow is that defined by the arithmetic mean of all grab samples, 77.5 ± 2.0 . The difference between this value and that of the chip mean is very small and the number of samples used to define it is greater. At a 90 percent confidence level there is a significant difference between the arithmetic mean of the four grab samples obtained from spheroidal zones in QTb₂ and both the grab sample mean of QTb₂ and the top position mean of QTb₂. At slightly

lower confidence levels of 89 and 82 percent the bottom position mean and the chip mean also exhibit significant differences from spheroidal zone samples. On the other hand, the middle position mean is similar to the spheroidal zone mean at all confidence levels greater than 59 percent.

The intensity of alteration and the composition of the olivine phenocryst fraction appear to be related. Areas of lower Fo content are areas of more intense alteration. The Fo content of phenocryst olivine is greatest in the top position mean, less in the bottom position mean, lesser in the middle position mean, and least in the mean defined by spheroidal zone samples. The intensity of alteration is inversely proportional since it is greatest in spheroidal zones and least in the top of the flow. Decrease in Fo content with intensity of alteration is thought to be due to a more active alteration of forsterite rich areas of phenocrysts by deuteric solutions which are retained in the central and spheroidal portions of the flow.

Grab samples from other basalt flows of the Parea Mesa, although not sampled extensively, do not differ significantly in phenocryst olivine composition from flow QTb₂. However, a limited number of samples from other localities in the state of New Mexico suggest that the olivine of the phenocryst fraction may vary from one olivine-bearing basalt to another.

Determination of olivine phenocryst compositions in olivine-bearing basalts may be of assistance in the study of this

rock type; the lack of variation in the composition of this mineral in a single flow may be of petrologic value. It may be that thicker or more extensive flows show variation in the olivine phenocryst composition in a lateral and/or a vertical sense. If the study of one flow can be used as an index for similar flows of the same general modal composition and thickness, the variation in compositional of olivine phenocrysts of relatively thin flows of olivine basalt is insignificant.

REFERENCES

- Allen, J. E. and Balk, R. (1954) Mineral resources of Fort Defiance and Tohatchi quadrangles, Arizona and New Mexico, N. Mex. Inst. of Mining and Tech., Bur. of Mines and Mineral Resources Bull. 36.
- Anonymous (1959) Science in the News, Geological Survey volcanologists study new series of eruptions at Hawaii's Kilauea, Science, 18 Dec., vol. 130, no. 3390, pp. 1695-1697.
- (1950) Tables for conversion of x-ray diffraction angles to interplanar spacing, Nat. Bur. of Std's, AMS 10.
- Bowen, N. L. (1928) The evolution of the igneous rocks, Princeton University Press.
- Brown, G. and Stephen, I. (1959) Structural study of iddingstite from New South Wales, Australia, Am. Mineral. vol. 44, pp. 251-260.
- Callaghan, E. and Sun, Ming-Shan (1956) Correlation of some igneous rocks of New Mexico by the Fusion Method, Trans., Amer. Geophy. Union vol. 37 No. 6, pp. 761-766.
- Darton, N. H. (1905) The Zuni Salt Lake, Jour. Geol. vol. 13, pp. 185-193.
- Fuller, R. E. (1931) The aqueous chilling of Basaltic Lava on the Columbia River Plateau, Am. Jour. Sc. vol. 21, pp. 281-300.
- (1938) Deuteric alteration controlled by the jointing of lavas, Am. Jour. Sc. vol. 35, pp. 160-171.

- Hack, J. T. (1942) Sedimentation and volcanism in the Hopi Buttes, Arizona, Geol. Soc. America, Bull. vol. 53, pp. 335-372.
- Hoel, P. G. (1947) Introduction to mathematical statistics, J. Wiley and Sons, Inc.
- Jicha, H. L., Jr. (1958) Geology and mineral resources of Mesa del Oro quadrangle, Socorro and Valencia Counties, New Mexico, N. Mex. Inst. of Mining and Tech., Bur. of Mines and Mineral Resources Bull. 56.
- Macdonald, G. A. (1944) The 1840 Eruption and crystal differentiation in the Kilauean magma column, Am. Jour. Sc., vol. 242, pp. 177-189.
- Mathews, W. H. (1951) A useful method for determining approximate composition of fine grained igneous rocks, Am. Mineral., vol. 36, pp. 92-109.
- Peacock, M. A. and Fuller, R. E. (1928) Chlorophæite, sideromelane, and pargasite from the Columbia River Plateau, Am. Mineral. vol. 13, pp. 361-369.
- Poldervaart, A. (1950) Correlation of physical properties and chemical composition in the plagioclase, olivine and orthopyroxene series, Am. Mineral. vol. 35, pp. 1067-1079.
- Rankama, K. and Sahama, T. G. (1950) Geochemistry, University of Chicago Press.
- Ringwood, A. E. (1958) The constitution of the mantle-I. Thermodynamics of the olivine-spinel transition, Geochim. et Cosmo. Acta, vol. 13, pp. 303-321.

- Russell, I. C. (1902) Geology and water resources of the Snake River Plains of Idaho, U. S. Geol. Survey Bull. 199, pp. 113-115.
- Sahama, T. G. and Torgeson, D. R. (1949) Some examples of the application of thermochemistry to petrology, Jour. Geol. vol. 57, pp. 255-262.
- Shoemaker, E. M. (1956) Occurrence of uranium in diatremes on the Navajo and Hopi Reservations, Arizona, New Mexico and Utah, U. S. Geol. Survey Prof. Paper 300, pp. 175-185.
- Sun, Ming-Shan (1957) The nature of iddingsite in some basaltic rocks of New Mexico, Am. Mineral. vol. 42, pp. 525-533.
- Wargo, J. G. (1960) Magnetic susceptibility and fusion data for some volcanic rocks from southwestern New Mexico, Geol. Soc. Am. vol. 77, no. 1, pp. 87-92.
- Weaver, G. E. (1956) The distribution and identification of mixed-layered clays in sedimentary rocks, Am. Mineral. vol. 41, pp. 202-221.
- Willard, Max E. and Weber, R. H. (1959) Reconnaissance Geologic Map of Canon Largo Thirty-Minute Quadrangle, Geologic Map 6, N. Mex. Inst. of Mining and Tech., State Bur. of Mines and Mineral Resources.
- Williams, H. (1936) Pliocene volcanoes of the Navajo-Hopi Country, Geol. Soc. America Bull. vol. 47 pp. 111-171.

Wilshire, H. G. (1958) Alteration of olivine and orthopyroxenes
in basic lavas and shallow intrusions, Am. Mineral., vol.
43, pp. 120-147.

Wright, H. E., Jr. (1946) Tertiary and Quaternary geology of the
lower Rio Puerco area, New Mexico, Geol. Soc. Am. vol.
57, pp. 383-456.

Yoder, H. S., Jr. and Sahama, T. G. (1957) Olivine x-ray determina-
tion curve, Am. Mineral. vol. 42, pp. 475-491.